Communications Biology

https://doi.org/10.1038/s42003-026-10156-5

Article in Press

Brain-heart interactions in late-onset major depressive disorder revealed by multimodal HRV-driven fMRI

Received: 11 October 2025

Accepted: 20 April 2026

Cite this article as: Goffi, F., Enrico, P., Reali, P. *et al.* Brain-heart interactions in late-onset major depressive disorder revealed by multimodal HRV-driven fMRI. *Commun Biol* (2026). https://doi.org/10.1038/s42003-026-10156-5

Federica Goffi, Paolo Enrico, Pierluigi Reali, Gabriele Torino, Maria Pia Marra, Lorena Di Consoli, Adele Ferro, Giandomenico Schiena, Yvan Torrente, Luciano Lombardi, Fabio M. Triulzi, Anna M. Bianchi, Paolo Brambilla & Eleonora Maggioni

Brain-heart interactions in late-onset major depressive disorder revealed by multimodal HRV-driven fMRI

Federica Goffi[1], Paolo Enrico[2], Pierluigi Reali[1], Gabriele Torino[2,3], Maria Pia Marra[2], Lorena Di Consoli[2], Adele Ferro[2], Giandomenico Schiena[2], Yvan Torrente[4,5], Luciano Lombardi[6], Fabio M. Triulzi[6], Anna M. Bianchi[1,7*], Paolo Brambilla[2,3^], Eleonora Maggioni[1,2^]

1 Department of Electronics Information and Bioengineering, Politecnico di Milano, Milan, Italy

2 Department of Neurosciences and Mental Health, Fondazione IRCCS Ca' Granda Ospedale Maggiore Policlinico, Milan, Italy

3 Department of Pathophysiology and Transplantation, Università degli Studi di Milano, Milan, Italy

4 Neurology Unit, Fondazione IRCCS Ca' Granda Ospedale Maggiore Policlinico, Milan, Italy

5 Stem Cell Laboratory, Dino Ferrari Center, Department of Pathophysiology and Trasplantation, Università degli Studi di Milano, Milan, Italy

6 Neuroradiology Unit, Fondazione IRCCS Ca' Granda Ospedale Maggiore Policlinico, Milan, Italy

7 Fondazione IRCCS Ca' Granda Ospedale Maggiore Policlinico, Milan, Italy

^ These authors jointly supervised this work

* Corresponding author

Corresponding author:

Anna Maria Bianchi
Department of Electronics Information and Bioengineering, Politecnico di Milano,
Piazza Leonardo da Vinci, 32, 20133, Milan, MI, Italy
Tel. +39 02 23993342. E-mail: annamaria.bianchi@polimi.it
https://orcid.org/0000-0002-8290-7460

Abstract

Major depressive disorder (MDD) is a heterogenous, systemic disease often associated with cardiac autonomic dysfunction, yet neurophysiological mechanisms linking altered autonomic regulation to brain function remain largely unexplored to date. Here, we investigate functional brain correlates of cardiac autonomic modulation in MDD by integrating heart rate variability (HRV) with brain functional magnetic resonance imaging (fMRI). Forty participants (20 late-onset MDD patients, 20 healthy controls) undergo simultaneous electrocardiography and resting-state fMRI. HRV-derived autonomic regressors representing low-frequency and parasympathetic activity are estimated using time-varying bivariate autoregressive modeling and used to drive voxel-wise fMRI analysis via a general linear model. Group-level analyses assess diagnosis effects controlling for age and sex. Post-hoc correlations are computed between HRV-related fMRI responses and clinical severity. Distinct patterns of brain-autonomic coupling emerge in MDD. Altered fMRI responses to autonomic dynamics are observed within central autonomic network regions, including insula, cingulate gyrus, and hippocampus. The right insula shows consistent hypoactivation across multiple autonomic contrasts, with its response negatively correlating with depression severity. These findings provide preliminary evidence of altered brain-autonomic integration in MDD, particularly within interoceptive, self-referential, and affective networks. HRV-fMRI integration emerges as a promising multimodal framework for identifying multi-organ markers of cardiac autonomic dysfunction in psychiatric disorders.

Keywords: heart rate variability; functional magnetic resonance imaging; brain-heart interplay; central autonomic network; major depressive disorder.

Introduction

Imagine the flutter of your heart in moments of excitement, or the calm you feel watching a sunset or gazing at the stars. These sensations are shaped by the intricate connection between the brain and the heart, a never-ending conversation between two of the body's most vital organs. This dynamic interplay, mediated through neural, hormonal, and electrical signals, not only sustains our physical health but also deeply influences emotional and cognitive states, playing a relevant role in mental health.

In recent years, alongside the increasing emphasis on molecular and genetic approaches to investigate biological mechanisms at the microscale, there has been a shift toward adopting a holistic perspective when studying diseases, focusing on the interconnectedness of the whole body rather than isolating a single organ[1]. Within this systemic perspective, the dynamic interplay between the brain and the heart has emerged as a critical yet still underexplored component in the understanding of the multi-morbid nature of psychiatric disorders, which are often accompanied by cardiovascular diseases (CVD)[2–4].

Major depressive disorder (MDD) provides a compelling context for investigating brain-heart interactions. MDD is a prevalent and disabling mental condition, affecting millions of adults worldwide, and it is increasingly recognized as a systemic disorder with heterogeneous etiology and symptomatology, including an elevated risk for cardiovascular morbidity and mortality[5–8]. Conversely, individuals with CVD frequently experience psychiatric complications[9]. A high prevalence of depression is observed in patients who have experienced stroke or major arrhythmia, underscoring the bidirectional nature of the brain-heart axis. Within these dynamics, the interoceptive experience – particularly the perception of cardiac signals – plays a pivotal communication role. Variations in heart function can influence how individuals perceive their internal state, which in turn may impact emotional regulation and cognitive processing [10,11]. The relationship between MDD and CVD is driven by a complex interplay of behavioral and biological mechanisms [8,12], among which altered cardiac autonomic regulation has been projected as an important pathophysiological factor [13–15]. Previous research has shown that the intrinsic

autonomic state of MDD is characterized by reduced autonomic control, mainly decreased parasympathetic vagal tone, which has been hypothesized as related to altered brain-level autonomic control [16–18].

The autonomic nervous system (ANS) plays a role in brain-heart communication[4,19–21]. A key non-invasive marker of ANS activity is the heart rate variability (HRV) that, measuring the beat-to-beat changes in heart rate (HR), reflects the balance between sympathetic (accelerating) and parasympathetic (decelerating) influences on the heart activity [22,23]. HRV oscillations occur across multiple frequency bands. The high-frequency (HF) component, usually synchronous with respiration, primarily reflects parasympathetic activity, whereas the low frequency (LF) component reflects mixed autonomic influences [24] and baroreflex mechanisms[25], while often increasing during sympathetic activation[26,27]. HR modulation via respiratory sinus arrhythmia (RSA), mostly represented in the HF range, is predominantly vagally mediated and provides a physiologically grounded marker of parasympathetic modulation[28,29]. HRV complexity arises from the coordinated and context-dependent synergy between these two branches, enabling adaptive responses to internal and environmental changes. According to the neurovisceral integration model [30–32], autonomic outflow to the heart is regulated by the central autonomic network (CAN), composed of interconnected cortical and subcortical structures across the telencephalon and diencephalon, which control the sympathetic outputs via preganglionic neurons in the brainstem vagal nuclei and in the spinal cord [33–35]. Key areas include the medial prefrontal cortex, insular cortex, the anterior cingulate cortex, and the amygdala, participating in autonomic control via descending outputs to the hypothalamus, and regions in the brainstem and medulla [4,33,36,37]. Alterations within this network are thought to link emotional dysregulation, cognitive control, and autonomic function – core features implicate in MDD psychopathology.

In the investigation of the still largely unknown heart-brain relationships in MDD, studies relying on single physiological parameters (e.g., HRV alone), such as previous work on cardiac sympatovagal

imbalance in MDD[16,18], can only provide limited information on hierarchically higher structures of the CAN, highlighting the importance of brain-level investigations[16]. A major challenge in studying brain-heart interactions lies in the current limited availability of data analysis methodologies able to reliably handle such information[38]. The difficulty stems not only from the distinct biological, chemical, and neural dynamics of the brain and heart, but also from the intricate physiological processes underlying their communication, which require equally sophisticated computational tools for analysis. Nevertheless, investigating integrated physiological systems offers the potential to move beyond organ-specific models toward a more comprehensive understanding of disorders involving multiple systems.

A substantial body of work has investigated brain-heart interactions using electroencephalography (EEG) combined with HRV measures, providing valuable insights into temporal relationships between peripheral autonomic signals and cortical activity[39]. EEG-HRV studies have been significant in characterizing fast neural processes associated with autonomic modulation and have informed theoretical models and therapeutic applications[40]. However, EEG-based approaches are intrinsically limited in spatial resolution and sensitivity to deep brain structures, which are thought to play a crucial role in autonomic regulation[33]. Functional magnetic resonance imaging (fMRI) offers complementary advantages by enabling the mapping of whole-brain activity with high spatial resolution and improved characterization of subcortical regions. It is based on the blood oxygen-level dependent (BOLD) contrast, used as hemodynamic proxy for the underlying local neural activity. Unimodal fMRI analyses have been instrumental in early CAN research, largely through task-based autonomic-eliciting paradigms[41]. Previously, neurophysiological information has been successfully used to guide fMRI analyses in other modalities (e.g., EEG-driven fMRI)[42,43], supporting the rationale for extending this strategy to cardiac autonomic signals. While technically challenging, the integration of HRV with fMRI allows a more data-driven characterization of CAN dynamics linked to peripheral autonomic control.

Although MDD is increasingly conceptualized as a disorder of the brain-heart axis, direct data-driven evidence of altered HRV-related dynamics within the CAN in MDD remains scarce, as highlighted in recent reviews emphasizing the need to characterize the brain-heart interplay not only in physiological conditions but also in the context of emotion dysregulation and depression[44,45]. Addressing this gap is essential for moving beyond a symptom-centered, brain-focused perspective toward a functional, whole-body framework for understanding and treating depression[44].

In the heterogeneous depression phenotype[46], late-onset MDD is increasingly recognized as a distinct clinical and neurobiological subtype of disease. Compared to early-onset forms, late-onset MDD is more frequently associated with altered aging mechanisms, including vascular dysregulation, increased cerebrovascular burden, and neurodegenerative processes, rather than predominantly psychosocial or genetic risk factors[47,48]. Importantly, late-onset MDD has been consistently associated with alterations in cardiovascular and autonomic regulation. Meta-analytic and longitudinal evidence indicates that older adults with depression exhibit reduced HRV, suggesting impaired autonomic flexibility and increased cardiovascular vulnerability[49,50]. These alterations occur in the context of age-related autonomic changes, including progressive reduction of parasympathetic modulation and altered sympathovagal balance, which may represent a biologically vulnerable substrate for depression in later life [51]. Together, these findings support late-onset MDD as a particularly informative model for investigating central mechanisms of brain-heart interaction, as age-related autonomic changes may interact with central regulatory mechanisms[52]. Disruptions in the brain-heart axis may represent a potential pathogenetic mechanism contributing specifically to the development or maintenance of late-onset MDD [44].

Within this context, the primary objective of the present study was to preliminarily explore resting-state brain-autonomic coupling in late-onset MDD using a multimodal HRV-fMRI integrated framework. By combining validated time-resolved modeling of HRV [53,54] and HRV-driven general linear model (GLM) fMRI approaches [55–57], we investigated the intrinsic brain hemodynamic and metabolic correlates of

cardiac autonomic variability using simultaneous electrocardiogram (ECG) and fMRI data acquired at rest. Our aim was to compare individuals with late-onset MDD and healthy controls (HC) in the brain regions whose activity covaries with autonomic dynamics, separating vagal (RSA) and non-vagal contributions. Based on existing theoretical and neurobiological evidence, we hypothesized that late-onset MDD would be characterized by alterations in HRV-related brain activity within key regions of the CAN, reflecting altered central regulation of cardiac autonomic dynamics. Given the involvement of large-scale resting-state networks in depression and their close relationship with autonomic and affective-cognitive processes, we further hypothesized these brain-autonomic alterations to spatially overlap with major intrinsic brain networks implicated in emotional regulation and cognitive control. These hypotheses were investigated within an exploratory, hypothesis-informed analytical framework. An overview of the multimodal framework integrating HRV and fMRI is illustrated in Figure 1.

By integrating peripheral autonomic dynamics with whole-brain fMRI, the present study adopts a data-driven but biologically grounded framework to investigate brain–heart interactions in late-onset MDD. Beyond advancing mechanistic understanding, characterizing central autonomic alterations may have translational relevance for treating depression, including neuromodulation-based interventions, such as vagus nerve stimulation and deep brain stimulation[58–60], which target circuits involved in autonomic and affective regulation. In this sense, the present work represents a first initial step toward identifying neurophysiological markers of altered brain–heart integration in depression and for targeted, potentially integrative, therapeutic interventions.

Figure 1.

Results

Sample demographic and clinical information

The sample included 40 participants, equally divided into 20 HC and 20 individuals diagnosed with late-onset MDD. Age distribution was comparable in MDD and HC groups (two sample t-test, $p>0.05$). Sex distribution was comparable between MDD and HC, given random association between males and females in the two groups (Chi-Square test, $p>0.05$).

The psychopathological assessment included the administration of the Hamilton Depression Rating Scale (HDRS) [61], the Depression Anxiety and Stress Scale-21 (DASS-21), divided into three constructs DASS-21 Depression (DASS-21-D), Anxiety (DASS-21-A) and Stress (DASS-21-S) [62], and the Traumatic Experience Checklist (TEC) [63]. Total HDRS scores were significantly higher in MDD patients than in HC (two sample t-test, $p<0.05$). DASS-21-A and DASS-21-S scores were not significantly different in the two groups (two sample t-test, $p>0.05$), whereas DASS-21-D scores were significantly higher in MDD patients (two sample t-test, $p<0.05$). TEC scores were higher in patients with MDD than in HC at trend level (two sample t-test, $p=0.0521$). The sample characteristics are summarized in Table 1.

Table 1.

HRV-driven fMRI analysis results

The HRV-driven fMRI analysis enabled the identification of brain regions with a significant BOLD response to non-vagal LF-related activity and vagal activity separately, and those differing between the two. In the following sections, the results are reported according to the different contrasts, as considered within the statistical parametric mapping design. Specifically, the next section reports the findings resulting from the comparison between HC and patients with MDD. Given our focus on this comparison,

the fMRI responses to HRV dynamics found in the entire group of subjects (at the net of sex, age, and diagnosis) are described in Supplementary Note 1 (Supplementary Figure 1-3; Supplementary Table 1-3). Briefly, group-level fMRI responses were observed in brain clusters belonging to the CAN, including the right anterior, middle, and posterior cingulate gyrus, right precuneus, left superior frontal gyrus, right supramarginal and postcentral gyrus, angular gyrus, and thalamus.

The brain clusters emerging from the comparison between groups were also used as regions of interest for exploratory functional connectivity analyses and post-hoc brain-clinical correlations.

MDD vs. HC

When comparing HRV-driven fMRI activation in MDD individuals compared to HC, controlling for age and sex, significant group differences in HRV-related BOLD response were observed across contrasts (Figure 2; Table 2). Considering LF-related activity modulation (i.e., non-RSA regressor), a significantly lower BOLD response in the MDD group than in HC one was found in the right anterior insula, right inferior temporal gyrus, vermis, right supramarginal and postcentral gyrus, left paraterminal gyrus, body of fornix, and brainstem (left inferior colliculus and periaqueductal gray, PAG). Specifically, an increase in non-RSA power in the LF band was reflected in a local fMRI activation that is significantly lower in patients with MDD than in HC in these brain regions.

Considering activation related to parasympathetic vagal activity (i.e., RSA regressor), right hippocampus and left precuneus showed significantly higher BOLD responses in individuals affected by MDD than in HC. Instead, in the HC group, a significantly higher BOLD response was found in the left cingulate gyrus (area cingularis anterior ventralis), right anterior insula, right cingulate gyrus (anterior cingulate agranular anterior limbic area), right cingulate gyrus (area cingularis anterior dorsalis), and cerebellum, suggesting that oxygenation, which is assumed to reflect neural activity, is decreased in these brain regions in MDD patients in relation to an increase in vagal activity modulation.

Considering sympatovagal balance (SVB) dynamics, a significantly higher BOLD response in MDD individuals than in HC was found in the right fusiform gyrus, right postcentral gyrus, and left inferior frontal gyrus, opercular part. A significantly lower BOLD response was found in the right posterior cingulate cortex in MDD patients than in HC.

In the non-RSA vs. RSA contrast, in MDD group compared to HC, significantly lower BOLD responses were found in the right anterior insula, right inferior temporal gyrus, right anterior central operculum, right postcentral and supramarginal gyrus, right fusiform gyrus, right temporo-occipital transition zone, left anterior insula (compact insular claustrum), right precuneus, vermis, right caudate nucleus, and right supramarginal gyrus.

Table 2.

Figure 2.

Results of HRV-driven seed-based functional connectivity analyses

Seed-to-voxel functional connectivity analyses were performed using as seeds the most significant clusters different between patients and controls in the previous HRV-driven fMRI analysis. The results suggest large-network alterations in late-onset MDD. Using the anterior insula identified in the non-RSA contrast as seed, MDD patients showed decreased connectivity with a set of regions predominantly involving sensorimotor, thalamic, fronto-parietal areas, and subcortical structures, including the nucleus accumbens and subgenual anterior cingulate cortex (sgACC). Using the hippocampal seed derived from the RSA-related contrast, patients with late-onset MDD showed increased functional connectivity with the right precuneus and reduced connectivity with a distributed set of subcortical, limbic, and sensorimotor regions, including hypothalamic subregions. Using the sgACC (BA25) seed derived from the negative RSA-related contrast, reduced functional connectivity was observed with multiple insular and

peri-insular regions. Additional results are reported in Supplementary Note 2 (Supplementary Figure 4; Supplementary Table 4-6).

Results of correlations between HRV-related fMRI responses and clinical scores

The significant results of the post-hoc partial correlation analyses between the HRV-related fMRI responses differing between MDD and HC and the clinical scores are reported in Table 3 ($p<0.05$). Both significant and trend-level level ($p<0.08$) findings are reported in Supplementary Note 3 (Supplementary Table 7).

Among the brain clusters with different fMRI responses to LF-related non-vagal modulation (non-RSA contrast) in the two groups, significant negative correlations between beta coefficients in the right inferior temporal gyrus and HDRS and between beta coefficients in the right insula and supramarginal/postcentral gyrus and DASS-21-D were found, suggesting an inverse relationship between the strength of the non-vagal LF-related-brain activity coupling in temporo-parietal clusters and depression severity. No significant correlations were found between TEC, DASS-21-A, and DASS-21-S scores and the peak beta coefficients of any of the non-RSA-related brain regions.

Among the brain clusters with different responses to vagal modulation (RSA contrast) in the two groups, a significant positive correlation was found between the beta coefficients in the right hippocampus and HDRS scores, meaning that higher depression severity was associated with higher BOLD response to vagal activity in this region. Instead, a negative correlation with both HDRS and DASS-21-D was found in the right insula, suggesting that higher depression severity is associated with lower vagal-insular coupling. No significant correlations were found between TEC, DASS-21-A, and DASS-21-S and the peak beta coefficients of any of the brain regions emerging for the RSA regressor. No significant correlations were found between clinical scores and the peak beta coefficients of any of the brain regions emerging as different between MDD and HC for the SVB regressor (only trend-level significant results).

For the non-RSA vs. RSA contrast, significant negative correlations between localized fMRI activations and depressive and stress symptoms were found. Specifically, a significant negative correlation was found between beta coefficients in the right inferior temporal gyrus, right anterior central operculum, left insula (compact insular claustrum), and right caudate, and HDRS scores. A negative correlation was found between the beta coefficients in the right insula and DASS-21-D. These findings suggest an inverse relationship between depressive symptomatology and the differential strength of the autonomic-brain coupling, meaning that increased depressive symptoms are associated with lower contrast between non-RSA and RSA-related brain activations, when differentially evaluated, in these regions. Also, a negative correlation was found between peak beta coefficients in the right supramarginal area and DASS-21-S, suggesting that greater stress is associated with lower contrast between non-RSA and RSA-related responses in this brain region. No significant correlations were found between TEC and DASS-21-A and the beta coefficients of any of the brain regions emerging for this contrast.

Table 3.

Discussion

In this exploratory study, we implemented a novel multimodal approach to investigate spontaneous interactions between brain activity and cardiac autonomic regulation. Simultaneous resting-state ECG–fMRI data were entered in an HRV-driven fMRI analysis, in which HRV information on non-vagal LF-related and parasympathetic dynamics was used to guide the fMRI analysis. This allowed us to identify brain regions that are involved in high-level central autonomic processes in an entirely data-driven framework and to investigate any differences between patients with late-onset MDD and controls. In our sample, fMRI responses were observed in regions pertaining to the CAN, supporting the physiological validity of our HRV-fMRI integrated approach.

For the first time, the application of this approach to patients with late-onset MDD revealed alterations in the central neural correlates of autonomic mechanisms within the CAN and in regions implicated in MDD psychopathology. While these results are novel and data-driven, the fact that altered HRV-related activity emerged in regions consistently implicated in autonomic regulation supports the reliability of the framework and its grounding in established neurophysiology. At the same time, given the exploratory nature of the study and the modest sample size, these results should be interpreted with appropriate caution and warrant replication in larger and independent cohorts. Post-hoc correlations were conducted as a secondary explorative follow-up analysis to provide additional descriptive insights into the relationship between altered HRV-BOLD coupling characterizing late-onset MDD and clinical symptom severity.

An integrated method for the study of brain-non-vagal and brain-vagal interactions

At the methodological level, our work supports the feasibility and added value of simultaneous ECG-fMRI acquisitions combined with subject-specific, inherently time-resolved autoregressive modeling to estimate autonomic dynamics and their cerebral correlates. With respect to currently available data

analysis techniques, the here-proposed methodological approach provides a suitable and up-to-date advanced framework for the investigation of brain functional correlates of non-vagal LF-related and parasympathetic activity, addressing both methodological and clinical needs previously highlighted [44].

Brain-heart interactions have been extensively studied using multimodal EEG-HRV approaches[39,64]. Owing to their superior temporal resolution, EEG-based studies have substantially contributed to characterizing the fast dynamics[65,66], complexity, and directionality of brain–heart interactions[67–71], as well as informing theoretical models and therapeutic applications[40]. In parallel, HRV–fMRI offers complementary strengths by enabling whole-brain coverage and a more detailed characterization of subcortical and limbic structures that play a central role in autonomic regulation but are difficult to resolve with scalp EEG[33,72]. EEG-HRV and HRV-fMRI should therefore be viewed as complementary, capturing different spatial and temporal aspects of brain-autonomic coupling. In this context, the present HRV-fMRI framework is particularly suited to investigating the brain correlates of autonomic dynamics in late-onset MDD, where subcortical, limbic, and vascular-related mechanisms are thought to play a prominent role.

Previous dynamic HRV-fMRI studies adopted an asymmetric approach, using HRV-derived metrics to guide the fMRI analysis in different conditions [55–57,73,74], typically based on multivariate voxel-level correlations with time-varying estimates of vagal activity, derived from heartbeat point-process modelling [75,76].

The framework proposed in this study belongs to the same category of methods (i.e, HRV-driven fMRI). The novelty of the present work lies primarily in its application to a unique late-onset MDD sample and in the integration of respiration-informed, time-resolved HRV modeling within an fMRI framework. The bivariate autoregressive model used here has been previously validated for characterizing HRV dynamics, and its integration within a physiology-informed GLM-based fMRI framework provides a mechanistic approach to identify neural circuits involved in autonomic regulation. A key methodological objective

was to improve the physiological specificity of LF-related HRV estimates compared to standard HRV approaches. To this end, we aimed to reduce known sources of variability by: (i) explicitly removing the HRV component that is coherent with respiration, thereby isolating LF variability not driven by RSA; and (ii) providing a more specific characterization of parasympathetic modulation by quantifying HF power that is coherent with RSA, rather than relying on broadband HF power alone. By accounting for respiratory contributions, the proposed framework enables a more physiologically grounded separation between vagal-related and non-vagal LF-related autonomic dynamics, offering complementary insight into central mechanisms of autonomic regulation (see Supplementary Note 4).

The findings obtained across the entire sample support the feasibility of our novel integrated approach, as significant BOLD responses to autonomic modulation were found within brain regions associated with the CAN, also considering an expansion of it with respect to the most traditional regions [41,55].

Importantly, the observed brain–autonomic coupling patterns were regionally specific rather than spatially diffuse, involving anatomically and functionally meaningful areas activated by autonomic-eliciting tasks, including experimental sympathetic challenges[41]. This spatial selectivity strengthens the biological plausibility of the identified effects. A more detailed discussion of group-level results is reported in Supplementary Note 1.

Clinical characteristics of the sample

MDD and HC groups were comparable in terms of age and sex, minimizing the influence of demographic confounds on the observed findings. As expected, individuals with late-onset MDD exhibited significantly higher depressive symptom severity compared to HC. No significant group differences were observed for anxiety and stress symptoms. Notably, depressive symptom severity in the present sample was on average mild, which may partially account for the absence of significant group differences in anxiety and stress measures. This pattern is consistent with the clinical profile of late-onset MDD, which is often

associated with lower anxiety comorbidity compared to early-onset or recurrent forms of depression [77,78]. In addition, lifetime traumatic experiences did not significantly differ between patients and controls, although a trend-level increase was observed in the MDD group. These clinical characteristics are relevant for interpreting the neuroimaging findings. Taken together, these features suggest that the observed alterations in brain–autonomic coupling are less likely to primarily reflect acute anxiety or stress-related states, or differential trauma exposure, and may instead index more stable, trait-like alterations in central autonomic regulation associated with late-onset depressive pathology.

Alterations in brain-autonomic coupling in depression

This study revealed significant differences in the functional brain correlates of autonomic control in patients with late-onset MDD, suggesting a potential relationship between cardiac autonomic alterations, particularly reduced parasympathetic tone as reported by unimodal HRV studies [16–18], and alterations in brain activity within key regions of the CAN. Early work combining HRV with regional cerebral blood flow measures demonstrated that autonomic alterations in depression are accompanied by changes in central physiological correlates [79]. The present study builds on this foundation by extending the investigation of brain–heart coupling to whole-brain, time-resolved HRV–fMRI analyses. Our findings of reduced coupling between brain activity and non-vagal LF-related dynamics in individuals with late-onset MDD may reflect impaired top-down regulation of sympathetic function. Based on this hypothesis, which cannot be tested using our fMRI dataset, this could result in diminished central-mediated sympathetic dynamics, thereby increasing the relative influence of peripheral regulatory mechanisms, such as baroreflex-mediated blood pressure control, on sympathetic activity modulation. Consequently, reduced HRV may derive from a shift toward more mechanically driven, reflex-based pathways (i.e., increased baroreflex dominance over centrally mediated autonomic modulation). Conversely, diminished central coupling with vagal efferent pathways may directly reduce

parasympathetic tone, further contributing to the observed decrease in HRV in MDD. This interpretation is particularly relevant in the context of late-onset MDD, where aging-related cardiovascular alterations may further compromise baroreflex sensitivity and autonomic flexibility [80]. Age-related changes in arterial compliance and blood pressure regulation may amplify the contribution of peripheral reflex mechanisms to sympathetic variability, especially when central autonomic regulation is weakened.

Significant reductions in the right insula activity to autonomic modulation were found across multiple contrasts in late-onset MDD. The insula is a core hub of the CAN [81–83] and plays a central role for interoceptive awareness [84] and in integrating autonomic signals with emotional and cognitive processes, constituting a pivotal node of the salience network [85,86]. In line with this functional role, reduced coupling between insular activity and cardiac autonomic dynamics — encompassing both vagal and non-vagal LF-related components — suggests impaired integration between central representations of bodily states and the actual peripheral autonomic signals. This interpretation is further supported by the observed associations with depressive symptom severity, as measured by HDRS and DASS-21-D scores, indicating that greater clinical burden may be linked to weaker insular–autonomic coupling. Hypoactivity of the insula has been consistently reported in MDD, particularly during tasks requiring attention to visceral sensations, suggesting a reduced involvement in processing interoceptive information [87]. Altered baseline activity of insula may thus represent a neural marker of interoceptive dysfunction in MDD, potentially leading to autonomic imbalance through abnormal representations of bodily signals. Specifically, impairments in heart-focused interoception (i.e., cardioception) have been proposed as a neural basis linking CVD and affective disorders [88]. In this context, the right insula has been identified as a key region in the cerebral regulation of cardiac function [89], further supporting its role in coordinating top-down and bottom-up interoceptive and autonomic processes. In line with this interpretation, previous MEG-based studies have reported altered coupling between HRV and fronto-insular activity in MDD and

deficits in inhibitory control, linking cardiac autonomic dysregulation also to reduced flexibility in higher-order cognitive processes [90].

Notably, reduced vagal-related coupling was also observed in the sgACC (BA25), a region that represents a principal site of autonomic regulation within the frontal lobe and has long been implicated in the neurovegetative symptoms of depression[91]. Previous work has provided converging evidence for a close relationship between BA25 activity and peripheral autonomic indices. BA25 activity has been reported to be negatively correlated with spontaneous skin conductance responses (an index of sympathetic arousal) during biofeedback paradigms [92,93] and to be positively correlated with cardiac vagal control, as in our study, during both emotional and cognitive tasks[94–96]. Specifically, Lane and colleagues demonstrated that BOLD signal changes within an *a priori* defined BA25 region of interest were significantly associated with vagal modulation changes during an emotional counting Stroop task in healthy participants, but not in individuals with MDD [97]. Also, Garcia and colleagues revealed mood- and sex-dependent interactions in the association between stress response circuitry activity and cardiovagal modulation in response to negative affective stimuli [98]. The present findings extend this literature by showing reduced vagal-related brain–heart coupling in BA25 using a data-driven, whole-brain HRV–fMRI framework. This suggests that altered sgACC–autonomic coupling in late-onset MDD may reflect a pervasive disruption of central autonomic regulation at rest, embedded within broader network-level alterations. Together, these results reinforce the view of sgACC as a critical hub at the interface between affective processing and parasympathetic regulation, with direct relevance for mechanistic models of depression and for neuromodulation approaches targeting brain–heart integration [60,99,100].

Key nodes of the default model network (DMN), including the precuneus, posterior cingulate gyrus, and hippocampus — regions that also overlap with the CAN — showed altered autonomic-related activation patterns in late-onset MDD. These regions are critically involved in self-referential thought and rumination, core features of depressive symptomatology [101]. The observed differences in MDD in HRV-

related activity within the DMN suggest a disrupted interplay between autonomic regulation function and intrinsic cognitive processes, potentially reflecting a reduced ability to flexibly regulate internally oriented attention and emotional processing in response to bodily changes. Consistent with this interpretation, hyperconnectivity within the DMN may reduce the network flexibility and impair its capacity to disengage other functions, which may extend to diminished responsiveness to autonomic demands.

Complementing the primary findings, somatosensory and sensorimotor regions, including the supramarginal and postcentral gyri, nodes of dorsal and ventral attention networks, showed altered HRV-driven activation in MDD. Although explorative, these findings are consistent with clinical observations of psychomotor retardation and altered somatosensory processing in depression [102]. Beyond interoception, proprioception is tightly linked to autonomic processes, and sympathetic activation is known to modulate somatosensory sensitivity[103]. In line with this, we found a lower coupling between the right postcentral gyrus activity and non-RSA-related BOLD response in MDD, suggesting a diminished control over LF-related HRV activity [104]. Furthermore, altered activation in the inferior temporal gyrus, a multisensory integration hub, may reflect disrupted sensory-affective integration, potentially contributing to altered perception and somatic symptoms commonly observed in depression [105]. Alterations involving the supramarginal gyrus further suggest disrupted somatosensory-affective integration, particularly in relation to stress. The observed association between reduced autonomic coupling in this region and perceived stress (DASS-21-S) aligns with prior evidence linking supramarginal gyrus alterations to chronic stress exposure and impaired emotional processing [106,107]. Chronic stress plays a crucial role in the central-autonomic communication and in MDD psychopathology[108], having a lasting influence on both psychological and physiological processes, potentially through epigenetic mechanisms [109–111].

Beyond these cortical regions, a broader set of limbic and subcortical structures exhibited altered HRV-related activity in late-onset MDD, including different subregions of the anterior and posterior cingulate cortices, compact insular claustrum (closely associated with the amygdala) [112], paraterminal gyrus [113], hippocampus, fornix [114,115], and caudate. These regions partly overlap with the CAN and limbic-affective networks and are critically involved in emotional regulation [116], stress responsivity [117], memory and homeostatic control. Engagement of brainstem regions further suggests dysregulation of primitive autonomic and defensive responses [118]. Rather than reflecting isolated regional abnormalities, these findings point to a distributed alteration in neurovisceral integration, whereby autonomic signals are processed and integrated across interconnected limbic, subcortical, and brainstem circuits. Altered coupling within these systems may reflect impaired coordination between autonomic regulation and emotional–cognitive processes.

From a theoretical perspective, these patterns may be interpreted within predictive processing and neural flexibility frameworks. Increased coupling in DMN regions involved in internal models, memory, and self-referential processing, together with reduced coupling in sensorimotor and interoceptive regions, may reflect an imbalance between top-down predictions and bottom-up bodily feedback [119]. Such a configuration could indicate a reduced influence of interoceptive and sensory prediction errors in refining autonomic regulation, consistent with altered neurovisceral integration and reduced physiological flexibility in MDD [120]. In line with neural flexibility hypotheses [121,122], increased engagement of default mode network regions involved in internal models may dominate sensory and interoceptive processing, potentially reducing the influence of bodily feedback on autonomic regulation [123]. These interpretations remain speculative and warrant future investigation using experimental designs specifically tailored to test predictive processing mechanisms.

Taken together, our preliminary findings suggest a widespread network-level alteration in how autonomic signals are integrated with large-scale brain systems implicated in cognition, emotion, and sensorimotor functions, potentially explaining the diverse and complex symptoms seen in MDD.

HRV-driven functional connectivity findings

Of note, these preliminary results suggested in a data-driven way the overlap between brain regions responsible for modulating autonomic functions (i.e., CAN) and those already acknowledged as implicated in the psychopathology of MDD [79,124,125], as illustrated in Figure 3 and Supplementary Figure 5. While such anatomical and functional overlap between CAN nodes and large-scale resting-state networks has been described in healthy populations, the present exploratory findings indicate that autonomic-related alterations and resting-state network changes may converge in late-onset MDD, highlighting a potentially novel aspect of brain–heart dysregulation in this condition.

Consistent with the current literature, the complexity and heterogeneity of depressive symptomatology may stem from the intricate alterations in functional connectivity both within and between large-scale brain networks. In MDD, altered connectivity affects networks responsible for processing internal (DMN) and external (dorsal attention network) stimuli, emotion and salience (affective and ventral attention networks, together referred to as salience network), and cognitive regulation (fronto-parietal network) [85,126,127]. These alterations may explain both emotional and cognitive impairments, as well as autonomic dysfunction, reinforcing the idea that MDD heterogeneous symptoms may share a common neurobiological basis rooted in altered neurovisceral integration.

In line with this view, our exploratory seed-based functional connectivity analyses suggest that regional alterations in HRV-related brain activity in late-onset MDD are embedded within broader network-level reconfigurations. Alterations primarily affected salience- and default-mode–related systems, suggesting disrupted integration between networks supporting interoceptive/autonomic processing and those

involved in internally oriented, self-referential cognition. This finding is aligned with previous work showing that older patients with depression exhibit altered functional connectivity between default mode and salience networks[128]. Additionally, posterior cingulate cortex and insula, important nodes of the DMN and salience network, respectively, were significantly associated with cardiovagal activity in women with higher depressed mode[129] . Functionally, this pattern is consistent with reduced salience-driven and sensorimotor integration alongside increased engagement of default mode regions, potentially reflecting an imbalance between bodily signal processing and internally generated representations.

Notably, these analyses revealed reduced functional connectivity between the anterior insula and sgACC (BA25) in late-onset MDD, providing mechanistic support for disrupted limbic–salience integration within central autonomic circuits and reinforcing the relevance of the sgACC as a neuromodulation target for deep brain stimulation in depression [59,60]. Moreover, increased vagal-related functional connectivity between the hippocampus and multiple hypothalamic areas was also observed in late-onset MDD, as also previously found in relationship with other central autonomic regions [129], suggesting alterations in stress response circuitry to coordinate homeostatic responses through modulation of cardiac autonomic and neuroendocrine signals. Such alterations further support disrupted neurovisceral integration in late-onset depression.

Brain-autonomic coupling and clinical implications in MDD

From a theoretical perspective, our findings suggesting impairments in central autonomic mechanisms in MDD, together with prior evidence of reduced HRV and altered cardiac autonomic regulation, are consistent with the neurovisceral integration model, which posits a close relationship between cognitive-emotional functioning and autonomic regulation [30–32]. Within this framework, adaptive functioning depends on the flexible and coordinated regulation of autonomic activity by central networks. Similarly,

polyvagal theory emphasizes that adaptive behavior is grounded in ANS functioning, whereby sympathetic activity regulates the “flight or fight” response while vagal activity is involved in higher-order responses associated with emotion regulation and social engagement. Importantly, adaptive functioning does not rely on the dominance of a single autonomic branch, but rather on the dynamic, coordinated and context-dependent interplay between sympathetic and parasympathetic influences, which together support flexible adaptation to internal and external demands [130–132]. The monitoring of visceral activity, with HRV as a marker of autonomic flexibility, is a key component of this adaptive process [133,134]. Low variability in HR reflects reduced flexibility in autonomic regulation, which may arise from increased sympathetic drive, reduced parasympathetic modulation, or altered integration between autonomic branches.

Conversely, higher HRV is generally associated with more efficient and flexible autonomic regulation, reflecting a greater capacity for dynamic vagal modulation within an integrated autonomic system, and is linked to enhanced self-regulation and adaptability [132,135,136]. In this view, reduced HRV in MDD may represent a physiological marker of impaired autonomic integration, self-regulation, and emotional processing. In line with this interpretation, the present study identifies corresponding alterations at the brain level, linking peripheral autonomic dynamics to activity within central networks implicated in autonomic and affective regulation.

Moreover, accumulating evidence highlights the strong interrelation between the ANS and immune function. Through vagal efferent pathways, the ANS modulates inflammatory responses via the cholinergic anti-inflammatory reflex, which inhibits pro-inflammatory cytokine release [137 138]. Reduced vagal tone, frequently reported in MDD, may therefore contribute to a pro-inflammatory state, supporting the hypothesis of shared pathophysiological pathways linking affective dysregulation and immune dysfunction. In this context, our findings of reduced brain–vagal coupling in late-onset MDD are consistent with weakened central regulation of autonomic and potentially inflammatory processes [139].

Altered activity in regions such as the insula and anterior cingulate gyrus, which represent hubs of both the CAN and neuroimmune axis, further suggests that impaired integration of interoceptive signals may contribute to the neurobiological interface between emotion, bodily awareness, and inflammation. Future studies integrating neuroimaging, HRV, and peripheral inflammatory markers may offer deeper insights into the complex brain–heart–immune interplay in MDD [140].

Finally, a comprehensive investigation of brain-heart interactions may offer novel and clinically relevant insights for advancing treatment strategies in MDD, particularly considering its high comorbidity with CVD and the substantial proportion of patients who do not respond to conventional treatments[141]. In this context, neuromodulation approaches, including non-invasive brain and vagal stimulation techniques, have shown promising antidepressant effects and may additionally improve autonomic regulation. Combined HRV-fMRI studies could be instrumental in optimizing such neuromodulation strategies by enabling the mapping of the fronto-vagal (brain-heart) pathway, ultimately tailoring interventions to restore both emotional and autonomic balance at cardiac level in MDD [58,142,143].

This exploratory work highlights the feasibility of HRV–fMRI integration in late-onset MDD and motivates future studies to test these hypotheses in larger samples. By incorporating quantitative assessments of brain–heart interplay, mental health care can move toward a more integrated, systems-level approach, aligning with practices already common in cardiology and neurology. This suggests the need to develop effective physiologically informed biomarkers of sympatovagal-related brain activity, which may also support the identification and characterization of specific MDD subgroups exhibiting autonomic dysfunction.

Figure 3.

Limitations

While this study provides preliminary insight into the functional coupling between autonomic and brain activity in late-onset MDD, some limitations should be acknowledged. First, the sample size was relatively modest, which may reduce the statistical power to detect subtle effects. Future studies with larger and more diverse cohorts are needed to validate and extend our results, improving the generalizability of the findings. Although MDD and HC groups were comparable in terms of age and sex, the older age of participants may have influenced both brain function and autonomic regulation independently of depression. We did not control for general medication use or lifestyle-related variables, which may have influenced both HRV and brain activity. In addition, the relatively mild average depressive symptom severity in the present cohort may limit generalizability to patients with more severe or heterogeneous depressive presentations, highlighting the need for future studies including a broader range of symptom intensity. From a more technical perspective, the study relied on ECG-derived respiration rather than direct respiratory measurements. While validated, this method may be less precise, particularly in capturing more complex breathing patterns that could influence vagal tone estimation. Finally, integrating systems with inherently different temporal dynamics and resolutions poses intrinsic challenges for temporal alignment and physiological interpretation, remaining a methodological limitation in multimodal integration.

The absence of formal correction for multiple comparisons represents a limitation of the present exploratory study, which however employed a conservative group-level GLM design framework. Replication in larger samples using more conservative correction strategies will be necessary to confirm the reported findings.

Post-hoc correlations between HRV-related brain-autonomic coupling and clinical symptom scores were exploratory and should be interpreted with caution, as correlations computed across diagnostic groups may be influenced by group separation and non-unimodal distributions of symptom severity.

In addition, these correlations relied on beta coefficients extracted from peak voxels of diagnosis-defined clusters; although clinical variables differed from the selection criterion, some degree of non-independence and effect size overestimation cannot be fully excluded. Future studies with larger samples and independently defined anatomical regions of interest will be required to confirm these exploratory associations. Despite these limitations, for the first time, the present study provides important preliminary evidence of altered brain-autonomic coupling in MDD and sets the stage for future investigations using larger samples, more refined control of confounds, and longitudinal designs. Going beyond the cross-sectional nature of the present study, in future works longitudinal and interventional designs are needed to explore causality and directionality of brain-autonomic interactions. Additionally, future developments will include integrated HRV-fMRI studies from functional and effective connectivity perspectives [144–146].

Conclusion

In the present study, an advanced integrated HRV-fMRI approach to investigate functional brain correlates of autonomic activity during resting state was presented. Our results support the feasibility and relevance of a multimodal HRV-driven fMRI analysis to investigate the central autonomic network in physiology and in late-onset MDD. From the HRV side, our method incorporated a continuous estimate of both non-vagal LF-related and vagal activities thanks to the use of time-varying bivariate autoregressive modeling. By integrating time-resolved estimates of autonomic activity with fMRI data acquired at rest, we identified distinct patterns of altered brain-autonomic coupling in late-onset MDD patients, particularly involving the insula, anterior cingulate cortex, hippocampus, precuneus, postcentral gyrus, and other subcortical regions. These findings suggest a dysfunctional interplay between autonomic regulation and brain function in depression, supporting the perspective of a shared neurobiological substrate underlying the heterogeneous and systemic symptomatology, potentially driven by altered neurovisceral integration. Importantly, these findings may also contribute to the identification and characterization of a potential MDD subgroup characterized by autonomic dysfunction driven by brain-level alterations.

Our multimodal data-driven approach highlights the potential of HRV-informed neuroimaging as a promising framework for identifying central markers of cardiac autonomic dysregulation, as well as for studying the potential for the adoption of therapeutic approaches that target the brain-heart axis to restore balance to autonomic regulation and improve mood and cognition. Future research should aim to replicate these findings in larger cohorts, examine their longitudinal stability, and explore their utility as biomarkers for diagnosis, prognosis, or treatment response in affective disorders.

Materials and Methods

Participants

The sample included in the present study consisted of 40 participants, divided into 20 healthy controls and 20 patients affected by late-onset MDD. Clinical diagnoses were assessed using the Italian version of the Structured Clinical Interview for DSM-5, Clinician Version (SCID-5-CV) [147]. Only subjects with late-onset MDD (≥ 45 years) were included in the patient group, and only subjects without lifetime psychiatric diagnoses were included in the control group. Exclusion criteria for patients were lifetime psychotic symptoms and current DSM-5 comorbid disorders. Exclusion criteria for all participants comprise lifetime alcohol or substance abuse, intellectual disability, history of head trauma with loss of consciousness, neurological or neurodegenerative illnesses. In MDD patients, information on age of illness onset and current pharmacological treatment was collected. All participants underwent a comprehensive cross-sectional evaluation by expert psychiatrists and psychologists, who were specifically trained for this recruitment. The psychopathological assessment included the administration of the Hamilton Depression Rating Scale (HDRS) [61], the Depression Anxiety and Stress Scale-21 (DASS-21), divided into three constructs DASS-21 Depression (DASS-21-D), Anxiety (DASS-21-A) and Stress (DASS-21-S) [62], and the Traumatic Experience Checklist (TEC) [63].

All subjects provided written informed consent to the study protocol. The study was conducted in accordance with the Declaration of Helsinki and approved by the Ethical Committee of Fondazione IRCCS Ca' Granda Ospedale Maggiore Policlinico, Milan, Italy (approval n. 238 2018bis). All ethical regulations relevant to human research participants were followed.

Data acquisition

All participants underwent a multimodal magnetic resonance imaging (MRI) session using a 3T Philips Achieva DStream scanner (Philips, Best, The Netherlands) equipped with a 32-channel head coil. Two hundred fMRI volumes (preceded by two dummy scans) were collected during resting wakefulness with eyes closed for 500 seconds using a multi-transmit T2*-weighted echo planar imaging (EPI) sequence (field of view (FOV): 120 mm (FH) × 256 mm (AP) × 256 mm (RL), voxel size: 2 × 2 × 2 mm^3, echo time (TE): 30 ms, repetition time (TR): 2500 ms, flip angle: 90°). During the fMRI session, simultaneous ECG recordings were performed using the MR-compatible Geodesic EEG System (GES400, Electrical Geodesic Inc., USA) equipped with a Hydrocel Geodesic Sensor Net (HCGSN v.1.0, Electrical Geodesic Inc., USA) including a single-lead ECG channel. The ECG sampling frequency was set at 1000 Hz. A structural brain image was acquired using a 3D T1-weighted turbo field echo (TFE) SENSE sequence (FOV: 250 mm (FH) × 240 mm (AP) × 180 mm (RL), voxel size: 1 x 1 x 1 mm^3, TE: 4 ms, TR: 8 ms, flip angle: 8°) and used as morphological reference for the fMRI analyses.

Participant inclusion based on data availability and quality

A total of 54 participants were initially recruited and underwent MRI scanning. Fourteen participants were excluded from the present analyses due to data availability or quality issues related to multimodal acquisition (attrition rate = 14/54 = 26%). Specifically, some participants lacked concurrent ECG recordings due to technical acquisition problems or the resting-state fMRI sequence, others were excluded due to poor-quality ECG signals unsuitable for HRV analysis, and others due to excessive head motion during fMRI acquisition, defined as a mean framewise displacement (FD) greater than 0.5 mm. The final sample included 40 participants.

fMRI data preprocessing

The preprocessing of structural and functional MRI data was performed by using HALFpipe toolbox [148]. The preprocessing pipeline within HALFpipe utilizes fMRIPrep [149], which includes skull stripping, brain tissue segmentation, and spatial normalization for structural images, and fMRI volumes realignment, coregistration with the anatomical image, and spatial normalization for functional images. Additional preprocessing steps were applied, including spatial smoothing with a full-width at half maximum (FWHM) of 6 mm, grand mean scaling, which sets the image mean – defined as the within-scan mean across all voxels and time points – to a predefined value (grand mean = 10,000), and Gaussian-weighted temporal filtering (FWHM = 125 s). The preprocessed fMRI data were resampled to the standard Montreal Neurological Institute (MNI) space, using the *MNI152NLin2009cAsym* template [150]. Based on a previous multi-metric comparison of different denoising strategies for resting-state fMRI data, which included both noise removal, signal of interest preservation and resting-state networks identifiability, the mean signal from white matter and cerebrospinal fluid, and the global signal were regressed out [151]. By doing this, widespread physiological fluctuations, including non-neural cardiac pulsation effects, were removed, whereas cardiac autonomic dynamics—associated with distinct neural processes—were explicitly modeled as regressors of interest, as described below.

ECG data preprocessing

ECG preprocessing was performed in MATLAB 2022b (MathWorks, Natick, MA, USA) using the EEGLAB toolbox [152] and in-house scripts. Gradient artifacts induced by the MRI environment were removed using a sliding average subtraction approach. Artifact templates were computed over 21 consecutive artifact blocks, each corresponding to one TR, and subtracted from the ECG signal with a step size of one TR [42,43,153,154]. The ECG signal was filtered with a band-pass Hamming windowed sinc FIR filter with cut-off frequencies of 0.1-120 Hz and a notch filter at 50 Hz to remove powerline interference and down

sampled to 250 Hz. R peaks were detected using the Pan-Tompkin's algorithm [155] and manually inspected and corrected. The tachogram was computed as the difference in time between consecutive R peaks. Respiration was estimated from the ECG using an ECG-derived respiration (EDR) approach [156,157]. Specifically, the preprocessed ECG signal was low-pass filtered using a Butterworth filter with a cut-off frequency of 0.5 or 1 Hz [156,158,159], depending on the individual characteristics, to isolate respiration-related baseline fluctuations associated with chest motion. The respirogram was then extracted by sampling the respiration in correspondence to each R peak [54,160]. The physiological plausibility of the EDR signal was verified by inspecting its power spectrum, which showed dominant peaks consistently within the typical respiratory frequency band for all participants. In addition, the estimated respiration rate fell within physiological resting-state limits across the sample. Additional methodological details are provided in Supplementary Note 5 (Supplementary Figure 6-10).

HRV regressors

Tachogram and respirogram were linearly detrended and inserted in a time-varying bivariate autoregressive model [54,161], which recursively adapts the model parameters using the least square method, with the introduction of a forgetting factor, and tracks the dynamical changes of the signals (see Supplementary Note 6; Supplementary Figure 11-12). This model enabled the cross-spectral analysis of the two signals in input, highlighting their linear frequency relationships in function of time [29,53,162]. The general equation of a bivariate autoregressive model of order p is:

$$Y(n) = \sum_{k=1}^{P} A(k)Y(n-k) + W(n)$$

$$Y(n) = \begin{bmatrix} y_1(n) \\ y_2(n) \end{bmatrix}, \quad A(k) = \begin{bmatrix} a_{11}(k) & a_{12}(k) \\ a_{21}(k) & a_{22}(k) \end{bmatrix}, \quad W(n) = \begin{bmatrix} w_1(n) \\ w_2(n) \end{bmatrix}$$

where $Y(n)$ presents the two signals, tachogram and respirogram, $A(k)$ are the p matrices of autoregressive parameters, and $W(n)$ is the vector of the residual terms. A model order p equal to 8 was selected, after inspecting the whiteness of the prediction error using the Ljung-Box Q-test applied to RR prediction residuals. Visual inspection of the normalized autocorrelation function was also performed to confirm the absence of systematic temporal structure. Additional details and illustrative examples on model order selection are reported in Supplementary Note 6 (Supplementary Figure 13-18; Supplementary Table 8-10). The forgetting factor, which allowed us to track the non-stationarities of the signals [163], was set to 0.98, then the parameters were estimated recursively using the Recursive Least Square (RLS) algorithm.

Starting from the estimated model coefficients, the power auto-spectra of both tachogram and respirogram were computed, as well as their cross-spectrum [164]. The tachogram spectrum was decomposed in two partial spectra. PSD12 describes the effect of y2 (respirogram) on y1 (tachogram), whereas PSD11 represents the residual amount of power, which is the power due to the only tachogram, and not the interaction between the two signals. Time-varying HRV parameters representing both sympathetic and vagal activity were computed to be later used as regressors in the fMRI analysis (section *Subject-level fMRI responses to HRV dynamics*). The regressor explaining sympathetic activity (referred to as non-RSA) was computed as the time-varying power integral in the LF range of PSD11, hence in the spectrum presenting the power of the tachogram itself. The time-varying power integral in PSD12 in the entire frequency range was computed and considered as the regressor reflecting parasympathetic activity (referred to as RSA). The power in this spectrum reflects the power in the tachogram due to respiration influence. In resting state, this interaction is mainly related to RSA physiological processes[165], reflecting contribution of vagal activity at the respiratory rate [23,28,29,162]. Additionally, a third regressor

was computed as the time varying sympatovagal balance (SVB), that is computed as the ratio between non-RSA (sympathetic) and RSA (vagal) power for each heartbeat. The power in the first two regressors was normalized to the total power, minus the power in the VLF band in PSD11. Formal validation of these measures against standard HRV indices was beyond the scope of the present study. Furthermore, PSD11 and PSD12 are time-resolved, model-based estimates of autonomic dynamics and are therefore not directly comparable to conventional stationary HRV metrics[23]. Rather, they provide complementary information on beat-to-beat cardiac autonomic regulation. Outlier removal on the three regressors was performed via Hampel identifier, which replaces any value in the time series that is more than three standard deviations from the median computed in a window composed of the sample and its six surrounding samples, three per side. The regressors were submitted to a centered moving average by sliding a window of three-sample length, comparable to the TR time interval of the fMRI. The convolution with the canonical hemodynamic response function was applied to each regressor to consider the intrinsic delay of the neurovascular coupling [166]. Finally, the time series were down sampled at the sampling frequency of the BOLD signals for the following integration with fMRI data.

HRV-driven fMRI analysis

The HRV-fMRI data analyses were carried out using SPM12 toolbox [167] in MATLAB and in-house scripts. After estimating the individual brain responses to HRV dynamics, the brain responses in the entire group and differing between HC and MDD groups were extracted. The altered brain responses observed in the patient group were further examined by assessing any correlations with clinical dimensions of interest. Further details on the abovementioned steps can be found in the following subsections.

Subject-level fMRI responses to HRV dynamics

The subject-level HRV and fMRI data were combined in an HRV-driven fMRI analysis to investigate the hemodynamic and metabolic brain correlates of cardiac autonomic variability. The resulting brain maps were entered into a group-level analysis to examine any relationships of fMRI responses with demographic and clinical factors. At the subject level, a general linear model (GLM) approach [168–170] was applied to identify brain regions exhibiting significant BOLD responses to non-vagal LF-related (non-RSA), vagal (RSA), and SVB dynamics, as represented by the three predefined HRV regressors. The design matrix included the non-RSA, RSA, and SVB regressors, along with the six motion parameters derived from the fMRI volumes realignment as non-interest regressors. After estimation of the GLM beta coefficients, statistical inference was performed by creating specific T contrasts to assess the contribution of each regressor of interest individually (non-RSA vs. baseline, RSA vs. baseline, and SVB vs. baseline) or in combination for the non-RSA vs. RSA contrast (computed as non-RSA minus RSA coefficients), to the overall BOLD signal. These contrasts were derived and entered one-by-one into the group-level analyses. In this multivariate framework, at the subject level, the fMRI correlates of the regressors of interest implicitly accounted for the contribution of the other regressors. Therefore, no correction for multiple contrasts were needed.

Group-level fMRI responses to HRV dynamics: the impact of diagnosis

At the group level, inference was made on the subject-level contrast maps representing the HRV-related fMRI correlates. Four group-level analyses were performed for non-RSA vs. baseline, RSA vs. baseline, SVB vs. baseline, and non-RSA vs. RSA contrast maps. The GLM design matrix for these analyses included age, sex, and diagnosis as regressors, plus a constant term used to evaluate the activation in the entire group at the net of the regressors. All group-level effects were estimated using a random-effects model, which is more conservative than traditional group-level fMRI analyses and supports population-level inference. Inference on group-level fMRI responses and diagnosis effects was based on T-contrasts on

the corresponding regressors. Given the exploratory nature of the study and the use of continuous, temporally variable physiological dynamics, statistical parametric maps were thresholded at a voxel-wise level of $p < 0.001$ (uncorrected), combined with a minimal cluster size threshold ($k = 3$ voxels). This approach was adopted to balance sensitivity and specificity in the context of subtle physiological effects, for which conventional voxel-wise or cluster-level family-wise error correction may be overly conservative given the reduced effect size expected for physiology-informed fMRI analyses.

The voxel clusters were subsequently labeled based on different atlases, including the Automated Anatomical Labeling (AAL) and the Paxinos & Mai Atlas of the Human Brain (fourth edition, 2015) [171,172]. The combined use of both atlases was intended to enhance anatomical precision, as the Paxinos & Mai atlas offers a more detailed delineation of small subcortical structures, which are particularly relevant for autonomic regulation. The term *central autonomic network* was used as a conceptual framework to interpret whether the anatomical location of significant clusters corresponded to brain regions implicated in autonomic regulation in the literature[33,72,173]. CAN regions were not defined a priori but considered post hoc for interpretative purposes.

Post-hoc functional connectivity analysis

To explore whether regional HRV-BOLD alterations in late-onset MDD might reflect broader network-level differences, we performed an exploratory seed-to-voxel resting-state functional connectivity analysis using representative seed regions extracted from the group-level HRV-driven fMRI alterations in MDD. Additional methodological details are provided in Supplementary Note 2.

Post-hoc correlations between HRV-related fMRI responses and clinical variables

In the brain clusters with significant differences between MDD patients and HC, explorative relationships between HRV-related fMRI responses and clinical scores were assessed by computing post-hoc partial

correlation analyses. Specifically, in the entire sample, partial correlations were computed between the subject-level GLM contrast coefficients (in the voxel with peak T values) and the scores for each clinical variable, while controlling for the influence of age and sex as additional covariates. The clinical variables consisted of HDRS, TEC, DASS-21-D, DASS-21-A, and DASS-21-S, resulting in five sets of partial correlation analyses. Statistical significance was set at $p<0.05$.

Data availability

Raw data were generated at Fondazione IRCCS Ca' Granda Ospedale Maggiore Policlinico, Milan, Italy. Data supporting the findings of this study are available upon request after signature of formal data transfer agreement.

Code availability

Custom scripts used for time-varying HRV estimation and HRV-fMRI integration have been deposited in an Open Science Framework (OSF) repository https://osf.io/7gp6y/?view_only=f44d17b1fdd3434fac1586cf7a09b75b.

References

1. Chen, W. G. *et al.* The Emerging Science of Interoception: Sensing, Integrating, Interpreting, and Regulating Signals within the Self. *Trends Neurosci* **44**, 3–16 (2021).
2. Craig, A. D. How do you feel? Interoception: the sense of the physiological condition of the body. *Nat Rev Neurosci* **3**, 655–666 (2002).
3. Samuels, M. A. The Brain–Heart Connection. *Circulation* **116**, 77–84 (2007).
4. Silvani, A., Calandra-Buonaura, G., Dampney, R. A. L. & Cortelli, P. Brain–heart interactions: physiology and clinical implications. *Philosophical Transactions of the Royal Society A: Mathematical, Physical and Engineering Sciences* **374**, 20150181 (2016).
5. Rabins, P. V., Harvis, K. & Koven, S. High fatality rates of late-life depression associated with cardiovascular disease. *J Affect Disord* **9**, 165–167 (1985).
6. Rajan, S. *et al.* Association of Symptoms of Depression With Cardiovascular Disease and Mortality in Low-, Middle-, and High-Income Countries. *JAMA Psychiatry* **77**, 1052–1063 (2020).
7. Shen, Q. *et al.* Psychiatric disorders and subsequent risk of cardiovascular disease: a longitudinal matched cohort study across three countries. *eClinicalMedicine* **61**, (2023).
8. Sowden, G. L. & Huffman, J. C. The impact of mental illness on cardiac outcomes: A review for the cardiologist. *International Journal of Cardiology* **132**, 30–37 (2009).
9. Liu, H., Luiten, P. G. M., Eisel, U. L. M., Dejongste, M. J. L. & Schoemaker, R. G. Depression after myocardial infarction: TNF-α-induced alterations of the blood–brain barrier and its putative therapeutic implications. *Neuroscience & Biobehavioral Reviews* **37**, 561–572 (2013).
10. Rae, C. L. *et al.* Impact of cardiac interoception cues and confidence on voluntary decisions to make or withhold action in an intentional inhibition task. *Sci Rep* **10**, 4184 (2020).

11. Schulz, S. M. Neural correlates of heart-focused interoception: a functional magnetic resonance imaging meta-analysis. *Philosophical Transactions of the Royal Society B: Biological Sciences* **371**, 20160018 (2016).
12. De Hert, M., Detraux, J. & Vancampfort, D. The intriguing relationship between coronary heart disease and mental disorders. *Dialogues Clin Neurosci* **20**, 31–40 (2018).
13. Bär, K.-J. *et al.* The influence of major depression and its treatment on heart rate variability and pupillary light reflex parameters. *Journal of Affective Disorders* **82**, 245–252 (2004).
14. Huffman, J. C., Celano, C. M., Beach, S. R., Motiwala, S. R. & Januzzi, J. L. Depression and cardiac disease: epidemiology, mechanisms, and diagnosis. *Cardiovasc Psychiatry Neurol* **2013**, 695925 (2013).
15. Jangpangi, D. Alteration of Heart Rate Variability in Patients of Depression. *JCDR* https://doi.org/10.7860/JCDR/2016/22882.9063 (2016) doi:10.7860/JCDR/2016/22882.9063.
16. Goffi, F., Maggioni, E., Bianchi, A. M., Brambilla, P. & Delvecchio, G. Is cardiac autonomic control affected in major depressive disorder? A systematic review of heart rate variability studies. *Transl Psychiatry* **15**, 217 (2025).
17. Kemp, A. H. *et al.* Impact of depression and antidepressant treatment on heart rate variability: a review and meta-analysis. *Biol Psychiatry* **67**, 1067–1074 (2010).
18. Koch, C., Wilhelm, M., Salzmann, S., Rief, W. & Euteneuer, F. A meta-analysis of heart rate variability in major depression. *Psychol Med* **49**, 1948–1957 (2019).
19. Coote, J. H. Myths and realities of the cardiac vagus. *J Physiol* **591**, 4073–4085 (2013).
20. Crick, S. J. *et al.* Innervation of the human cardiac conduction system. A quantitative immunohistochemical and histochemical study. *Circulation* **89**, 1697–1708 (1994).
21. Sunagawa, K., Kawada, T. & Nakahara, T. Dynamic nonlinear vago-sympathetic interaction in regulating heart rate. *Heart Vessels* **13**, 157–174 (1998).

22. Heart rate variability: standards of measurement, physiological interpretation and clinical use. Task Force of the European Society of Cardiology and the North American Society of Pacing and Electrophysiology. *Circulation* **93**, 1043–1065 (1996).
23. Shaffer, F. & Ginsberg, J. P. An Overview of Heart Rate Variability Metrics and Norms. *Front Public Health* **5**, 258 (2017).
24. Valenza, G., Citi, L., Saul, J. P. & Barbieri, R. Measures of sympathetic and parasympathetic autonomic outflow from heartbeat dynamics. *J Appl Physiol (1985)* **125**, 19–39 (2018).
25. Billman, G. E. The LF/HF ratio does not accurately measure cardiac sympatho-vagal balance. *Front. Physiol.* **4**, (2013).
26. Montano, N. *et al.* Power spectrum analysis of heart rate variability to assess the changes in sympathovagal balance during graded orthostatic tilt. *Circulation* **90**, 1826–1831 (1994).
27. van de Borne, P., Montano, N., Pagani, M., Oren, R. & Somers, V. K. Absence of low-frequency variability of sympathetic nerve activity in severe heart failure. *Circulation* **95**, 1449–1454 (1997).
28. Grossman, P. & Taylor, E. W. Toward understanding respiratory sinus arrhythmia: relations to cardiac vagal tone, evolution and biobehavioral functions. *Biol Psychol* **74**, 263–285 (2007).
29. Reali, P. *et al.* Assessing stress variations in children during the strange situation procedure: comparison of three widely used respiratory sinus arrhythmia estimation methods. *Physiol Meas* **42**, (2021).
30. Thayer, J. F., Hansen, A. L., Saus-Rose, E. & Johnsen, B. H. Heart rate variability, prefrontal neural function, and cognitive performance: the neurovisceral integration perspective on self-regulation, adaptation, and health. *Ann Behav Med* **37**, 141–153 (2009).
31. Thayer, J. F. & Lane, R. D. A model of neurovisceral integration in emotion regulation and dysregulation. *J Affect Disord* **61**, 201–216 (2000).

32. Thayer, J. F. & Lane, R. D. Claude Bernard and the heart-brain connection: further elaboration of a model of neurovisceral integration. *Neurosci Biobehav Rev* **33**, 81–88 (2009).
33. Benarroch, E. E. The central autonomic network: functional organization, dysfunction, and perspective. *Mayo Clin Proc* **68**, 988–1001 (1993).
34. Benarroch, E. E. The clinical approach to autonomic failure in neurological disorders. *Nat Rev Neurol* **10**, 396–407 (2014).
35. Lamotte, G., Shouman, K. & Benarroch, E. E. Stress and central autonomic network. *Autonomic Neuroscience* **235**, 102870 (2021).
36. Cechetto, D. F. Cortical control of the autonomic nervous system. *Experimental Physiology* **99**, 326–331 (2014).
37. Lane, R. D. Neural substrates of implicit and explicit emotional processes: a unifying framework for psychosomatic medicine. *Psychosom Med* **70**, 214–231 (2008).
38. Valenza, G., Toschi, N. & Barbieri, R. Uncovering brain-heart information through advanced signal and image processing. *Philos Trans A Math Phys Eng Sci* **374**, 20160020 (2016).
39. Candia-Rivera, D., Faes, L., De Vico Fallani, F. & Chavez, M. Measures and Models of Brain-Heart Interactions. *IEEE Rev Biomed Eng* **PP**, (2025).
40. Sezer, I. *et al.* Enhanced Brain-Heart Connectivity as a Precursor of Reduced State Anxiety after Therapeutic Virtual Reality Immersion. *Advanced Science* **12**, e03606 (2025).
41. Sklerov, M., Dayan, E. & Browner, N. Functional neuroimaging of the central autonomic network: recent developments and clinical implications. *Clin Auton Res* **29**, 555–566 (2019).
42. Bondi, E. *et al.* Neurovascular coupling of inhibitory control in late-onset depression: a simultaneous EEG-fMRI study. *NeuroImage* **317**, 121320 (2025).

43. Maggioni, E. *et al.* Investigation of the electrophysiological correlates of negative BOLD response during intermittent photic stimulation: An EEG-fMRI study. *Human Brain Mapping* **37**, 2247–2262 (2016).
44. Valenza, G. Depression as a cardiovascular disorder: central-autonomic network, brain-heart axis, and vagal perspectives of low mood. *Front. Netw. Physiol.* **3**, (2023).
45. Blickle, M. *et al.* Heart rate variability, interoceptive accuracy and functional connectivity in middle-aged and older patients with depression. *J Psychiatr Res* **170**, 122–129 (2024).
46. Tassi, E. *et al.* Gene–environment–brain topology reveals clinical subtypes of depression in UK Biobank. *Sci Rep* **15**, 35538 (2025).
47. Bukh, J. D., Bock, C., Vinberg, M., Gether, U. & Kessing, L. V. Differences between early and late onset adult depression. *Clin Pract Epidemiol Ment Health* **7**, 140–147 (2011).
48. Fiske, A., Wetherell, J. L. & Gatz, M. Depression in older adults. *Annu Rev Clin Psychol* **5**, 363–389 (2009).
49. Rouch, I. *et al.* Association between depressive symptoms and long-term heart rate variability in older women: Findings from a population-based cohort. *J Affect Disord* **305**, 151–158 (2022).
50. Brown, L. *et al.* Heart rate variability alterations in late life depression: A meta-analysis. *J Affect Disord* **235**, 456–466 (2018).
51. Stein, P. K., Barzilay, J. I., Chaves, P. H. M., Domitrovich, P. P. & Gottdiener, J. S. Heart rate variability and its changes over 5 years in older adults. *Age Ageing* **38**, 212–218 (2009).
52. Fahim, M. A., Yao, Y., Tipparaju, S. M. & Xuan, W. The heart-brain crosstalk in age related cardiovascular and neurodegenerative diseases. *Fluids Barriers CNS* **22**, 89 (2025).
53. Steyde, G., Calcagno, A., Reali, P. & Bianchi, A. M. Quantitative measures of autonomic activations during software development. in *2022 IEEE 21st Mediterranean Electrotechnical Conference (MELECON)* 574–578 (2022). doi:10.1109/MELECON53508.2022.9842918.

54. Bianchi, A. *et al.* Spectral analysis of heart rate variability signal and respiration in diabetic subjects. *Med Biol Eng Comput* **28**, 205–211 (1990).

55. Valenza, G. *et al.* The central autonomic network at rest: Uncovering functional MRI correlates of time-varying autonomic outflow. *Neuroimage* **197**, 383–390 (2019).

56. Sclocco, R. *et al.* Brain Circuitry Supporting Multi-Organ Autonomic Outflow in Response to Nausea. *Cereb Cortex* **26**, 485–497 (2016).

57. Napadow, V. *et al.* Brain correlates of autonomic modulation: combining heart rate variability with fMRI. *Neuroimage* **42**, 169–177 (2008).

58. Iseger, T. A., van Bueren, N. E. R., Kenemans, J. L., Gevirtz, R. & Arns, M. A frontal-vagal network theory for Major Depressive Disorder: Implications for optimizing neuromodulation techniques. *Brain Stimul* **13**, 1–9 (2020).

59. Xu, E. *et al.* Neural interoceptive processing is modulated by deep brain stimulation to subcallosal cingulate cortex for treatment-resistant depression. *Biological Psychiatry: Cognitive Neuroscience and Neuroimaging* **10**, 495–503 (2025).

60. Mayberg, H. S. *et al.* Deep brain stimulation for treatment-resistant depression. *Neuron* **45**, 651–660 (2005).

61. Hamilton, M. A rating scale for depression. *J Neurol Neurosurg Psychiatry* **23**, 56–62 (1960).

62. Lovibond, P. F. & Lovibond, S. H. The structure of negative emotional states: comparison of the Depression Anxiety Stress Scales (DASS) with the Beck Depression and Anxiety Inventories. *Behav Res Ther* **33**, 335–343 (1995).

63. Nijenhuis, E. R. S., Van der Hart, O. & Kruger, K. The psychometric characteristics of the Traumatic Experiences Checklist (TEC): First findings among psychiatric outpatients. *Clinical Psychology & Psychotherapy* **9**, 200–210 (2002).

64. Sadoun, S. N., Boutin, A., Cottin, F. & Laleg-Kirati, T.-M. Modeling Brain-Heart Interaction: A Review of Mechanistic Dynamical Models. *IEEE Rev Biomed Eng* **PP**, (2025).

65. Sargent, K. *et al.* Brain–body dysconnectivity: deficient autonomic regulation of cortical function in first-episode schizophrenia. *Psychological Medicine* **55**, e1 (2025).

66. Sargent, K. S. *et al.* Oscillatory Coupling Between Neural and Cardiac Rhythms. *Psychol Sci* **35**, 517–528 (2024).

67. Candia-Rivera, D., Catrambone, V., Barbieri, R. & Valenza, G. Functional assessment of bidirectional cortical and peripheral neural control on heartbeat dynamics: A brain-heart study on thermal stress. *Neuroimage* **251**, 119023 (2022).

68. Candia-Rivera, D. Modeling brain-heart interactions from Poincaré plot-derived measures of sympathetic-vagal activity. *MethodsX* **10**, 102116 (2023).

69. Catrambone, V. & Valenza, G. Nervous-System-Wise Functional Estimation of Directed Brain-Heart Interplay Through Microstate Occurrences. *IEEE Trans Biomed Eng* **70**, 2270–2278 (2023).

70. Catrambone, V., Greco, A., Vanello, N., Scilingo, E. P. & Valenza, G. Time-Resolved Directional Brain-Heart Interplay Measurement Through Synthetic Data Generation Models. *Ann Biomed Eng* **47**, 1479–1489 (2019).

71. Faes, L., Marinazzo, D., Jurysta, F. & Nollo, G. Linear and non-linear brain-heart and brain-brain interactions during sleep. *Physiol Meas* **36**, 683–698 (2015).

72. Beissner, F., Meissner, K., Bär, K.-J. & Napadow, V. The autonomic brain: an activation likelihood estimation meta-analysis for central processing of autonomic function. *J Neurosci* **33**, 10503–10511 (2013).

73. Miedema, M. *et al.* Modelling the effect of cardiac and respiratory fluctuations on the central autonomic network in a novel test-retest dataset. *NeuroImage* 121369 (2025) doi:10.1016/j.neuroimage.2025.121369.

74. Bolender, A. *et al.* Altered parasympathetic outflow and central sensitization response to continuous pain in cyclic vomiting syndrome: a functional magnetic resonance imaging study. *American Journal of Physiology-Gastrointestinal and Liver Physiology* **328**, G125–G135 (2025).

75. Barbieri, R., Matten, E. C., Alabi, A. A. & Brown, E. N. A point-process model of human heartbeat intervals: new definitions of heart rate and heart rate variability. *Am J Physiol Heart Circ Physiol* **288**, H424-435 (2005).

76. Barbieri, R. & Brown, E. N. Analysis of heartbeat dynamics by point process adaptive filtering. *IEEE Trans Biomed Eng* **53**, 4–12 (2006).

77. Baldwin, R. C. & Tomenson, B. Depression in later life. A comparison of symptoms and risk factors in early and late onset cases. *Br J Psychiatry* **167**, 649–652 (1995).

78. Janssen, J., Beekman, A. T. F., Comijs, H. C., Deeg, D. J. H. & Heeren, T. J. Late-life depression: the differences between early- and late-onset illness in a community-based sample. *Int J Geriatr Psychiatry* **21**, 86–93 (2006).

79. Nugent, A. C., Bain, E. E., Thayer, J. F., Sollers, J. J. & Drevets, W. C. Heart rate variability during motor and cognitive tasks in females with major depressive disorder. *Psychiatry Res* **191**, 1–8 (2011).

80. Monahan, K. D. Effect of aging on baroreflex function in humans. *American Journal of Physiology-Regulatory, Integrative and Comparative Physiology* **293**, R3–R12 (2007).

81. Benarroch, E. E. Insular cortex. *Neurology* **93**, 932–938 (2019).

82. Critchley, H. D. Neural mechanisms of autonomic, affective, and cognitive integration. *J Comp Neurol* **493**, 154–166 (2005).

83. Oppenheimer, S. & Cechetto, D. The Insular Cortex and the Regulation of Cardiac Function. *Compr Physiol* **6**, 1081–1133 (2016).

84. (Bud) Craig & D, A. How do you feel — now? The anterior insula and human awareness. *Nat Rev Neurosci* **10**, 59–70 (2009).

85. Menon, V. Large-scale brain networks and psychopathology: a unifying triple network model. *Trends in Cognitive Sciences* **15**, 483–506 (2011).

86. Seeley, W. W. The Salience Network: A Neural System for Perceiving and Responding to Homeostatic Demands. *J. Neurosci.* **39**, 9878–9882 (2019).

87. Hu, L. *et al.* Insular dysfunction of interoception in major depressive disorder: from the perspective of neuroimaging. *Front Psychiatry* **14**, 1273439 (2023).

88. Khalsa, S. S. & Lapidus, R. C. Can Interoception Improve the Pragmatic Search for Biomarkers in Psychiatry? *Front. Psychiatry* **7**, (2016).

89. Leopold, C. & Schandry, R. The heartbeat-evoked brain potential in patients suffering from diabetic neuropathy and in healthy control persons. *Clin Neurophysiol* **112**, 674–682 (2001).

90. Zhou, H. *et al.* Decreased Task-Related HRV Is Associated With Inhibitory Dysfunction Through Functional Inter-Region Connectivity of PFC in Major Depressive Disorder. *Front. Psychiatry* **10**, (2020).

91. Drevets, W. C., Savitz, J. & Trimble, M. The subgenual anterior cingulate cortex in mood disorders. *CNS Spectr* **13**, 663–681 (2008).

92. Critchley, H. D., Elliott, R., Mathias, C. J. & Dolan, R. J. Neural activity relating to generation and representation of galvanic skin conductance responses: a functional magnetic resonance imaging study. *J Neurosci* **20**, 3033–3040 (2000).

93. Critchley, H. D. Electrodermal responses: what happens in the brain. *Neuroscientist* **8**, 132–142 (2002).

94. Thayer, J. F., Ahs, F., Fredrikson, M., Sollers, J. J. & Wager, T. D. A meta-analysis of heart rate variability and neuroimaging studies: implications for heart rate variability as a marker of stress and health. *Neurosci Biobehav Rev* **36**, 747–756 (2012).

95. Rose, E. J., Simonotto, E. & Ebmeier, K. P. Limbic over-activity in depression during preserved performance on the *n*-back task. *NeuroImage* **29**, 203–215 (2006).

96. Critchley, H. D. *et al.* Human cingulate cortex and autonomic control: converging neuroimaging and clinical evidence. *Brain* **126**, 2139–2152 (2003).

97. Lane, R. D. *et al.* Subgenual anterior cingulate cortex activity covariation with cardiac vagal control is altered in depression. *Journal of Affective Disorders* **150**, 565–570 (2013).

98. Garcia, R. G. *et al.* Impact of sex and depressed mood on the central regulation of cardiac autonomic function. *Neuropsychopharmacol.* **45**, 1280–1288 (2020).

99. Schwartz, J. *et al.* Resting-state functional connectivity and inflexibility of daily emotions in major depression. *J Affect Disord* **249**, 26–34 (2019).

100. Hamani, C. *et al.* The subcallosal cingulate gyrus in the context of major depression. *Biol Psychiatry* **69**, 301–308 (2011).

101. Sheline, Y. I. *et al.* The default mode network and self-referential processes in depression. *Proc Natl Acad Sci U S A* **106**, 1942–1947 (2009).

102. Ray, D., Bezmaternykh, D., Mel'nikov, M., Friston, K. J. & Das, M. Altered effective connectivity in sensorimotor cortices is a signature of severity and clinical course in depression. *Proc Natl Acad Sci U S A* **118**, e2105730118 (2021).

103. Chu, B., Marwaha, K., Sanvictores, T., Awosika, A. O. & Ayers, D. Physiology, Stress Reaction. in *StatPearls* (StatPearls Publishing, Treasure Island (FL), 2025).

104. Kropf, E., Syan, S. K., Minuzzi, L. & Frey, B. N. From anatomy to function: the role of the somatosensory cortex in emotional regulation. *Braz J Psychiatry* **41**, 261–269 (2019).

105. Kapfhammer, H.-P. Somatic symptoms in depression. *Dialogues Clin Neurosci* **8**, 227–239 (2006).

106. Guo, Y. *et al.* Stress and the brain: Emotional support mediates the association between myelination in the right supramarginal gyrus and perceived chronic stress. *Neurobiol Stress* **22**, 100511 (2023).

107. Sokołowski, A., Folkierska-Żukowska, M., Jednoróg, K., Moodie, C. A. & Dragan, W. Ł. The relationship between early and recent life stress and emotional expression processing: A functional connectivity study. *Cogn Affect Behav Neurosci* **20**, 588–603 (2020).

108. Thayer, J. F. & Sternberg, E. M. Neural aspects of immunomodulation: focus on the vagus nerve. *Brain Behav Immun* **24**, 1223–1228 (2010).

109. Infurna, M. R. *et al.* Associations between depression and specific childhood experiences of abuse and neglect: A meta-analysis. *J Affect Disord* **190**, 47–55 (2016).

110. Mandelli, L., Petrelli, C. & Serretti, A. The role of specific early trauma in adult depression: A meta-analysis of published literature. Childhood trauma and adult depression. *Eur Psychiatry* **30**, 665–680 (2015).

111. Silva, R. C., Maffioletti, E., Gennarelli, M., Baune, B. T. & Minelli, A. Biological correlates of early life stressful events in major depressive disorder. *Psychoneuroendocrinology* **125**, 105103 (2021).

112. Druga, R. Chapter 2 - The Structure and Connections of the Claustrum. in *The Claustrum* (eds Smythies, J. R., Edelstein, L. R. & Ramachandran, V. S.) 29–84 (Academic Press, San Diego, 2014). doi:10.1016/B978-0-12-404566-8.00002-7.

113. Barany, L. *et al.* Topographical anatomy of the septum verum and its white matter connections. *Sci Rep* **14**, 18064 (2024).

114. Kamali, A. *et al.* The Cortico-Limbo-Thalamo-Cortical Circuits: An Update to the Original Papez Circuit of the Human Limbic System. *Brain Topography* **36**, 371 (2023).

115. Benear, S. L., Ngo, C. T. & Olson, I. R. Dissecting the Fornix in Basic Memory Processes and Neuropsychiatric Disease: A Review. *Brain Connectivity* **10**, 331 (2020).

116. Heimer, L. & Van Hoesen, G. W. The limbic lobe and its output channels: implications for emotional functions and adaptive behavior. *Neurosci Biobehav Rev* **30**, 126–147 (2006).

117. Kim, J. J. & Diamond, D. M. The stressed hippocampus, synaptic plasticity and lost memories. *Nat Rev Neurosci* **3**, 453–462 (2002).

118. Benarroch, E. E. Periaqueductal gray. *Neurology* **78**, 210–217 (2012).

119. Barrett, L. F. & Simmons, W. K. Interoceptive predictions in the brain. *Nat Rev Neurosci* **16**, 419–429 (2015).

120. Ullsperger, M., Harsay, H. A., Wessel, J. R. & Ridderinkhof, K. R. Conscious perception of errors and its relation to the anterior insula. *Brain Struct Funct* **214**, 629–643 (2010).

121. Uddin, L. Q. Cognitive and behavioural flexibility: neural mechanisms and clinical considerations. *Nat Rev Neurosci* **22**, 167–179 (2021).

122. Stange, J. P., Alloy, L. B. & Fresco, D. M. Inflexibility as a Vulnerability to Depression: A Systematic Qualitative Review. *Clin Psychol (New York)* **24**, 245–276 (2017).

123. Doss, M. K. *et al.* Psilocybin therapy increases cognitive and neural flexibility in patients with major depressive disorder. *Transl Psychiatry* **11**, 574 (2021).

124. Thayer, J. Brain and vagus nerve stimulation: a neurovisceral integration perspective. *Brain Stimulation: Basic, Translational, and Clinical Research in Neuromodulation* **14**, 1750 (2021).

125. Cattarinussi, G., Delvecchio, G., Maggioni, E., Bressi, C. & Brambilla, P. Ultra-high field imaging in Major Depressive Disorder: a review of structural and functional studies. *Journal of Affective Disorders* **290**, 65–73 (2021).

126. Kaiser, R. H., Andrews-Hanna, J. R., Wager, T. D. & Pizzagalli, D. A. Large-Scale Network Dysfunction in Major Depressive Disorder: A Meta-analysis of Resting-State Functional Connectivity. *JAMA Psychiatry* **72**, 603–611 (2015).

127. Bondi, E., Maggioni, E., Brambilla, P. & Delvecchio, G. A systematic review on the potential use of machine learning to classify major depressive disorder from healthy controls using resting state fMRI measures. *Neuroscience & Biobehavioral Reviews* **144**, 104972 (2023).

128. Blickle, M. *et al.* Heart rate variability, interoceptive accuracy and functional connectivity in middle-aged and older patients with depression. *Journal of Psychiatric Research* **170**, 122–129 (2024).

129. Garcia, R. G. *et al.* Impact of sex and depressed mood on the central regulation of cardiac autonomic function. *Neuropsychopharmacol.* **45**, 1280–1288 (2020).

130. Porges, S. W. The polyvagal theory: phylogenetic substrates of a social nervous system. *Int J Psychophysiol* **42**, 123–146 (2001).

131. Porges, S. W. The polyvagal perspective. *Biological Psychology* **74**, 116–143 (2007).

132. Porges, S. W. The polyvagal theory: New insights into adaptive reactions of the autonomic nervous system. *Cleve Clin J Med* **76**, S86–S90 (2009).

133. Candia-Rivera, D. Brain-heart interactions in the neurobiology of consciousness. *Current Research in Neurobiology* **3**, 100050 (2022).

134. Öhman, A. & Wiens, S. On the automaticity of autonomic responses in emotion: An evolutionary perspective. in *Handbook of affective sciences* 256–275 (Oxford University Press, New York, NY, US, 2003).

135. McCraty, R. & Shaffer, F. Heart Rate Variability: New Perspectives on Physiological Mechanisms, Assessment of Self-regulatory Capacity, and Health risk. *Glob Adv Health Med* **4**, 46–61 (2015).

136. Shaffer, F., McCraty, R. & Zerr, C. L. A healthy heart is not a metronome: an integrative review of the heart's anatomy and heart rate variability. *Front Psychol* **5**, 1040 (2014).

137. Tracey, K. J. The inflammatory reflex. *Nature* **420**, 853–859 (2002).

138. Thayer, J. F. Vagal tone and the inflammatory reflex. *Cleve Clin J Med* **76 Suppl 2**, S23-26 (2009).

139. Abohashem, S. *et al.* Depression and Anxiety Associate With Adverse Cardiovascular Events via Neural, Autonomic, and Inflammatory Pathways. *Circulation: Cardiovascular Imaging* **19**, e017706 (2026).

140. Aronica, R., Enrico, P., Squarcina, L., Brambilla, P. & Delvecchio, G. Association between Diffusion Tensor Imaging, inflammation and immunological alterations in unipolar and bipolar depression: A review. *Neuroscience & Biobehavioral Reviews* **143**, 104922 (2022).

141. Zhdanava, M. *et al.* The Prevalence and National Burden of Treatment-Resistant Depression and Major Depressive Disorder in the United States. *J Clin Psychiatry* **82**, 20m13699 (2021).

142. Iseger, T. A., Padberg, F., Kenemans, J. L., Gevirtz, R. & Arns, M. Neuro-Cardiac-Guided TMS (NCG-TMS): Probing DLPFC-sgACC-vagus nerve connectivity using heart rate - First results. *Brain Stimul* **10**, 1006–1008 (2017).

143. Garcia, R. G. *et al.* Respiratory-Gated Auricular Vagal Afferent Nerve Stimulation (RAVANS) Modulates Brain Response to Stress in Major Depression. *J Psychiatr Res* **142**, 188–197 (2021).

144. Duggento, A. *et al.* Globally conditioned Granger causality in brain-brain and brain-heart interactions: a combined heart rate variability/ultra-high-field (7 T) functional magnetic resonance imaging study. *Philos Trans A Math Phys Eng Sci* **374**, 20150185 (2016).

145. Goffi, F. *et al.* Data-driven Discovery of the Central Autonomic Network: Dynamic Integration of HRV and Multivariate fMRI Connectivity. in *2024 46th Annual International Conference of the IEEE Engineering in Medicine and Biology Society (EMBC)* 1–5 (2024). doi:10.1109/EMBC53108.2024.10782925.

146. Goffi, F. *et al.* An HRV-fMRI-DTI Integrated Framework at Ultra-High Magnetic Field. in *2024 IEEE International Conference on Metrology for eXtended Reality, Artificial Intelligence and Neural Engineering (MetroXRAINE)* 1100–1105 (2024). doi:10.1109/MetroXRAINE62247.2024.10795924.

147. Structured Clinical Interview for the DSM (SCID) - First - Major Reference Works - Wiley Online Library. https://onlinelibrary.wiley.com/doi/10.1002/9781118625392.wbecp351.

148. Waller, L. *et al.* ENIGMA HALFpipe: Interactive, reproducible, and efficient analysis for resting-state and task-based fMRI data. *Hum Brain Mapp* **43**, 2727–2742 (2022).

149. Esteban, O. *et al.* fMRIPrep: a robust preprocessing pipeline for functional MRI. *Nat Methods* **16**, 111–116 (2019).

150. Horn, A. MNI T1 6thGen NLIN to MNI 2009b NLIN ANTs transform. figshare https://doi.org/10.6084/m9.figshare.3502238.v2 (2016).

151. Goffi, F., Bianchi, A. M., Schiena, G., Brambilla, P. & Maggioni, E. Multi-Metric Approach for the Comparison of Denoising Techniques for Resting-State fMRI. *Human Brain Mapping* **46**, e70080 (2025).

152. Delorme, A. & Makeig, S. EEGLAB: an open source toolbox for analysis of single-trial EEG dynamics including independent component analysis. *J Neurosci Methods* **134**, 9–21 (2004).

153. Allen, P. J., Josephs, O. & Turner, R. A Method for Removing Imaging Artifact from Continuous EEG Recorded during Functional MRI. *NeuroImage* **12**, 230–239 (2000).

154. Maggioni, E. *et al.* Removal of pulse artefact from EEG data recorded in MR environment at 3T. Setting of ICA parameters for marking artefactual components: application to resting-state data. *PLoS One* **9**, e112147 (2014).

155. Pan, J. & Tompkins, W. J. A Real-Time QRS Detection Algorithm. *IEEE Transactions on Biomedical Engineering* **BME-32**, 230–236 (1985).

156. Bailón, R., Sörnmo, L. & Laguna, P. ECG-Derived Respiratory Frequency Estimation. in (2007).

157. O'Brien, C. & Heneghan, C. A comparison of algorithms for estimation of a respiratory signal from the surface electrocardiogram. *Computers in Biology and Medicine* **37**, 305–314 (2007).

158. Sharma, H., Sharma, K. K. & Bhagat, O. L. Respiratory rate extraction from single-lead ECG using homomorphic filtering. *Computers in Biology and Medicine* **59**, 80–86 (2015).

159. Varon, C. *et al.* A Comparative Study of ECG-derived Respiration in Ambulatory Monitoring using the Single-lead ECG. *Sci Rep* **10**, 5704 (2020).

160. Baselli, G., Cerutti, S., Civardi, S., Malliani, A. & Pagani, M. Cardiovascular variability signals: towards the identification of a closed-loop model of the neural control mechanisms. *IEEE Trans Biomed Eng* **35**, 1033–1046 (1988).

161. Mainardi, L. T. *et al.* Multivariate time-variant identification of cardiovascular variability signals: a beat-to-beat spectral parameter estimation in vasovagal syncope. *IEEE Trans Biomed Eng* **44**, 978–989 (1997).

162. Coelli, S., De Tommaso, M., Reali, P., Actis-Grosso, R. & Bianchi, A. M. Modulation of autonomic responses to cognitive tasks under acute mental stress. *Sci Rep* **16**, 4878 (2026).

163. Bianchi, A. M. *et al.* Time-variant power spectrum analysis for the detection of transient episodes in HRV signal. *IEEE Transactions on Biomedical Engineering* **40**, 136–144 (1993).

164. Baselli, G. *et al.* Spectral and cross-spectral analysis of heart rate and arterial blood pressure variability signals. *Comput Biomed Res* **19**, 520–534 (1986).

165. Yasuma, F. & Hayano, J.-I. Respiratory sinus arrhythmia: why does the heartbeat synchronize with respiratory rhythm? *Chest* **125**, 683–690 (2004).

166. Friston, K. J., Josephs, O., Rees, G. & Turner, R. Nonlinear event-related responses in fMRI. *Magn Reson Med* **39**, 41–52 (1998).

167. Friston, K. J. *Statistical Parametric Mapping: The Analysis of Functional Brain Images*. (Elsevier / Academic Press, Amsterdam Boston, 2007).

168. Hansen, K. A., David, S. V. & Gallant, J. L. Parametric reverse correlation reveals spatial linearity of retinotopic human V1 BOLD response. *Neuroimage* **23**, 233–241 (2004).

169. Monti, M. M. Statistical Analysis of fMRI Time-Series: A Critical Review of the GLM Approach. *Front Hum Neurosci* **5**, 28 (2011).

170. Poline, J.-B. & Brett, M. The general linear model and fMRI: does love last forever? *Neuroimage* **62**, 871–880 (2012).

171. *Atlas of the Human Brain*. (2015).

172. Tzourio-Mazoyer, N. *et al.* Automated anatomical labeling of activations in SPM using a macroscopic anatomical parcellation of the MNI MRI single-subject brain. *Neuroimage* **15**, 273–289 (2002).

173. Critchley, H. D., Nagai, Y., Gray, M. A. & Mathias, C. J. Dissecting axes of autonomic control in humans: Insights from neuroimaging. *Auton Neurosci* **161**, 34–42 (2011).

Funding

FG and EM were partly supported by the European Union – Next Generation EU (PRIN 2022 PNRR, grant n. P20229MFRC).

GT was supported by the ERA-NET NEURON JTC 2023 (RESILNET), grant n. NEURON RV-117 (ERP-2023-23684211 – FINANZ. RMIN512 - CUP C43C24001170002 - COD. PROG. MI-0142).

PB was partially supported by grants from the Italian Ministry of Education and Research - MUR ('Dipartimenti di Eccellenza' Programme 2023–27 - Dept. of Pathophysiology and Transplantation, Università degli Studi di Milano), the Italian Ministry of Health (Project "Hub Life Science" - Diagnostica Avanzata, HLS-DA, PNC-E3-2022-23683266– CUP: C43C22001630001 / MI-0117 / Piano Nazionale Complementare Ecosistema Innovativo della Salute; Ricerca Corrente 2026), by the ERANET Neuron JTC 2023 (ERP-2023-23684211 - ResilNet) and Eranet Neuron JTC 2024 (ER-2024-23684536 - BRAWO Project).

YT is funded by Unmet Medical Needs, Fondazione Regionale per la Ricerca Biomedica (FRRB-2022; Project REMODEL, PR-0490, CDC/CDR 230R16), Cariplo Telethon Alliance GJC2021-2022 (Project # GJC21084), Piano nazionale di ripresa e resilienza (PNRR), NextGenerationEU and MUR (National Center for Gene Therapy and Drugs based on RNA Technology, Spoke #1: Genetic diseases, PNRR CN3 RNA, 2022), Gruppo familiari beta-sarcoglicanopatie (GFB-ONLUS, Project PR-0394), INNOVA, Italian network of excellence for advanced diagnosis, PNC-E3-2022-23683266 PNC-HLS-DA CUP C43C22001630001, Associazione Centro Dino Ferrari.

Author Contributions

FG: Conceptualization, Methodology, Software, Formal Analysis, Investigation, Validation, Data Curation, Visualization, Writing – Original Draft, Writing – Review & Editing; PE: Conceptualization, Investigation, Validation, Resources, Writing – Review & Editing; PR: Methodology, Software, Validation, Writing –

Review & Editing; GT: Investigation, Resources, Writing – Review & Editing; MPM: Resources, Writing – Review & Editing; LDC: Resources, Writing – Review & Editing; AF: Resources, Writing – Review & Editing; GS: Resources, Writing – Review & Editing; YT: Resources, Writing – Review & Editing; LL: Investigation, Resources, Data Curation, Writing – Review & Editing; FMT: Resources, Writing – Review & Editing; AMB: Conceptualization, Methodology, Validation, Supervision, Writing – Review & Editing; PB: Resources, Writing – Review & Editing, Supervision, Project Administration, Funding acquisition; EM: Conceptualization, Methodology, Validation, Investigation, Writing – Review & Editing, Visualization, Supervision, Project administration, Funding Acquisition.

Competing interests

The authors declare no competing interests.

Figures

Figure 1. Overview of the analysis workflow, including unimodal fMRI and HRV analyses, and HRV-driven fMRI within a multimodal integration framework. Created in BioRender. Goffi, F. (2026) https://BioRender.com/gjjkvt0 (fMRI, functional magnetic resonance imaging; R, R peaks; BOLD, blood oxygenation level-dependent; ANS, autonomic nervous system; RSA, respiratory sinus arrhythmia; SVB, sympathovagal balance; HRV, heart rate variability; GLM, general linear model; MDD, major depressive disorder; HC, healthy controls).

Figure 2. Brain regions showing significant HRV-related BOLD response differences between patients with MDD and HC. Axial slices are displayed for each contrast: (A) non-RSA regressor; (B) RSA regressor; (C) SVB regressor; (D) non-RSA vs. RSA contrast. Red indicates MDD > HC; blue indicates MDD < HC (ITG, inferior temporal gyrus; PTG, paraterminal gyrus; SMG, supramarginal gyrus; PoG, postcentral gyrus; aCG, anterior cingulate gyrus; mCG, middle cingulate gyrus; FuG, fusiform gyrus; pCG, posterior cingulate gyrus; IFGop, inferior frontal gyrus (opercular part); Temp–Occ, temporo-occipital transition area; aOp, anterior central operculum.

Figure 3. Overlap between HRV-related brain activations, resting-state networks, and the central autonomic network in patients with MDD compared with HC. Panels show regions with significant group differences: (A) non-RSA-related activations; (B) RSA-related activations. Red dots indicate MDD > HC; blue dots indicate MDD < HC. (C) Reference map of major resting-state networks and the central autonomic network (light green, frontoparietal network; pink, default mode network; yellow, ventral attention network; red, affective (affective and ventral attention networks, together referred to as salience network); light blue, dorsal attention network; dark green, central autonomic network (PTG, paraterminal gyrus; SMG, supramarginal gyrus; PoG, postcentral gyrus; aCG, anterior cingulate gyrus; mCG, middle cingulate gyrus).

Tables

Table 1. Demographic and clinical characteristics of the study sample.

	HC	MDD	Stats (HC vs. MDD)
Participants (n)	20	20	-
Age (years)	69.9 ± 10.8	66.2 ± 7.7	T = 1.24, p = 0.22
Sex (F/M)	13/7	9/11	χ^2 = 1.62, p = 0.20
HDRS	2.2 ± 3.9	9.9 ± 5.9	T = -4.82, p = 2.29e-05*
DASS-21-A	4.1 ± 3.8	5.3 ± 7.1	T = -0.67, p = 0.51
DASS-21-S	10.4 ± 6.9	13.5 ± 10.2	T = -1.13, p = 0.26
DASS-21-D	5.4 ± 7.1	11.5 ± 10.1	T = -2.22, p = 0.032*
TEC	9.9 ± 5.8	14.8 ± 8.9	T = -2.01, p = 0.052

Continuous variables are reported as mean ± SD (SD, standard deviation; F, females; M, males; MDD, major depressive disorder; HC, healthy controls; HDRS, Hamilton depression rating scale; DASS-21-A, Depression Anxiety Stress Scale 21 – Anxiety; DASS-21-S, Depression Anxiety Stress Scale 21 – Stress; DASS-21-D, Depression Anxiety Stress Scale 21 – Depression; TEC, Traumatic Experience Checklist). *p < 0.05.

Table 2. Brain regions showing significant BOLD response for each contrast (non-RSA, RSA, SVB, and non-RSA vs. RSA).

Contrast	Effect	Brain region	k	p-value	Peak T	MNI coordinates (x, y, z)
non-RSA	**MDD < HC**	Anterior insula R	23	5.33e-06	5.11	40, -0, 10
		Inferior temporal gyrus R (BA20)	11	4.31e-05	4.42	46, -48, -12
		Vermis	4	1.17e-04	4.10	-2, -54, -6
		Supramarginal / Postcentral gyrus R	8	2.71e-04	3.80	32, -32, 42
		Paraterminal gyrus L (BA25)	3	4.79e-04	3.60	-2, 6, 2
		Body of fornix L	3	5.41e-04	3.55	-6, -26, 24
		Brainstem – inferior colliculus L / PAG	3	6.46e-04	3.49	-6, -36, -10
RSA	**MDD > HC**	Hippocampus R	10	1.86e-05	4.70	38, -40, -2
		Precuneus L (BA31)	3	2.88e-04	3.78	-10, -46, 52

	MDD < HC	Cingulate gyrus L (area cingularis anterior ventralis, BA24)	4	1.06e-04	4.12	-2, -14, 50
		Anterior insula R	8	2.08e-04	3.89	38, 2, 8
		Cingulate gyrus R (anterior cingulate agranular anterior limbic area, OP24, BA25)	3	3.00e-04	3.76	6, 24, -4
		Cingulate gyrus R (area cingularis anterior dorsalis, BA32)	5	3.59e-04	3.70	8, 8, 46
		Cerebellum	5	4.36e-04	3.63	12, -50, -22
SVB	**MDD > HC**	Fusiform gyrus R (BA20)	5	2.31e-04	3.85	44, -46, -16
		Postcentral gyrus R (BA3)	3	2.97e-04	3.76	22, -26, 74
		Inferior frontal gyrus, opercular part L (BA44)	4	3.14e-04	3.75	-50, 10, 22
	MDD < HC	Posterior cingulate gyrus R	4	4.34e-04	3.63	12, -42, 6
non-RSA vs. RSA	**MDD < HC**	Anterior insula R	14	2.03e-05	4.67	40, -0, 10
		Inferior temporal gyrus R (BA20)	13	2.99e-05	4.54	46, -50, -12
		Anterior central operculum R (BA43)	7	4.62e-05	4.40	54, -16, 18
		Postcentral gyrus / Supramarginal gyrus R (BA40)	22	7.31e-05	4.25	38, -34, 40
		Fusiform gyrus R (BA37)	3	1.28e-04	4.05	26, -70, -6
		Temporo-occipital transition zone R (BA37)	9	1.29e-04	4.05	42, -74, 14
		Anterior insula L (compact insular claustrum)	5	1.62e-04	3.98	-30, 10, 18
		Precuneus R	6	2.25e-04	3.86	12, -66, 52
		Vermis	3	3.77e-04	3.68	-2, -54, -6
		Caudate nucleus R	4	3.80e-04	3.68	18, -10, 26
		Supramarginal gyrus R (BA40)	7	4.30e-04	3.64	64, -24, 38

Clusters showing significant group differences (MDD vs. HC) are reported for each contrast. Coordinates are given in MNI space. k = cluster size (number of voxels); Peak T = maximum t-value within the cluster. Statistical threshold: voxel-wise $p < 0.001$ (MDD, major depressive disorder; HC, healthy controls; BA, Brodmann area; PAG, periaqueductal gray).

Table 3. Correlation between cluster peak beta values and clinical measures.

Contrast	Clinical measure	Brain region	ρ	p-value
non-RSA	**HDRS**	Inferior temporal gyrus R	-0.342	0.0356
	DASS-21-D	Anterior insula R	-0.370	0.0222
		Supramarginal / Postcentral gyrus R	-0.392	0.0150
RSA	**HDRS**	Hippocampus R	+0.460	0.0037
		Anterior insula R	-0.325	0.0465
	DASS-21-D	Anterior insula R	-0.347	0.0329
non-RSA vs. RSA	**HDRS**	Inferior temporal gyrus R	-0.412	0.0101
		Anterior central operculum R	-0.426	0.0076
		Anterior insula L (compact insular claustrum)	-0.443	0.0053
		Caudate nucleus R	-0.415	0.0096
	DASS-21-D	Anterior insula R	-0.337	0.0386
	DASS-21-S	Supramarginal gyrus R	-0.358	0.0275

Correlations (ρ) between beta values extracted at cluster peaks and clinical measures are reported (HDRS, Hamilton depression rating scale; DASS-21-S, Depression Anxiety Stress Scale 21 – Stress; DASS-21-D, Depression Anxiety Stress Scale 21 – Depression).

Editor Summary

Integration of HRV and fMRI reveals altered brain-autonomic coupling in late-onset major depressive disorder, particularly within the central autonomic regions, default mode and salience networks.

Peer Review Information

Communications Biology thanks Susan Whitfield-Gabrieli and the other, anonymous, reviewer(s) for their contribution to the peer review of this work. Primary Handling Editor: Benjamin Bessieres. A peer review file is available.

Background

Late-onset major depressive disorder (MDD)

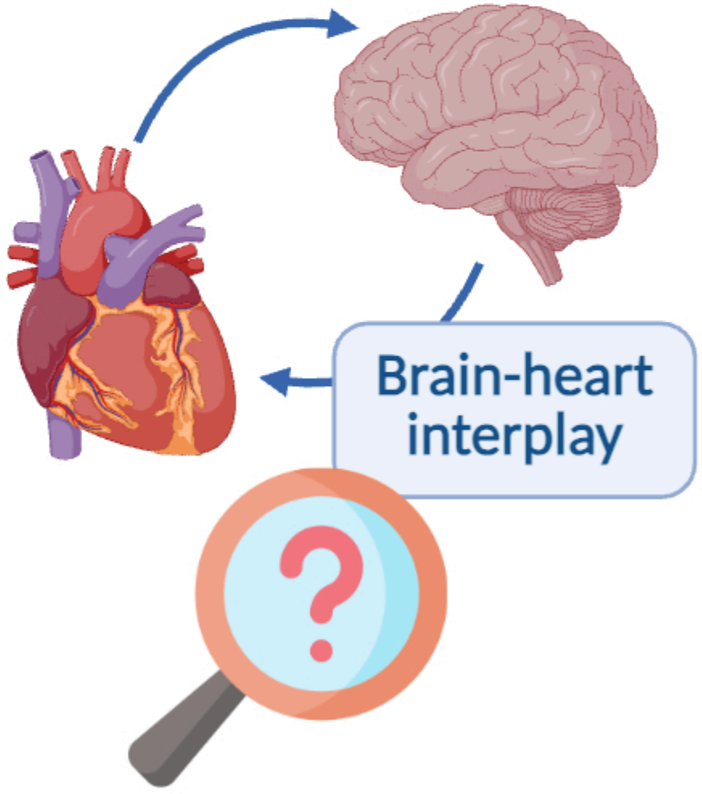

Brain-heart interplay

Methodological approach

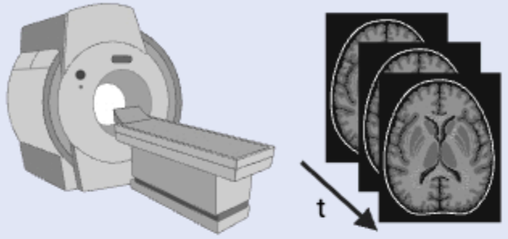

functional MRI data

ECG and HRV data

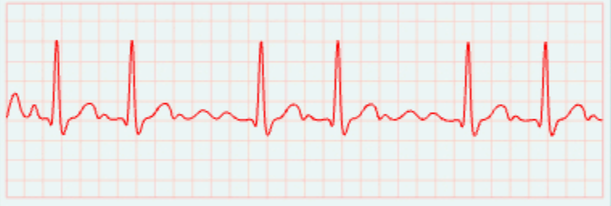

Multimodal HRV-fMRI integration

Results & Impact

fMRI responses to vagal and non-vagal HRV dynamics

MDD vs. HC

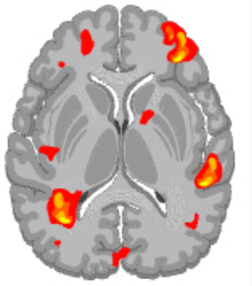

Clusters of the central autonomic network

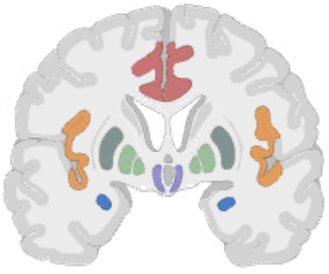

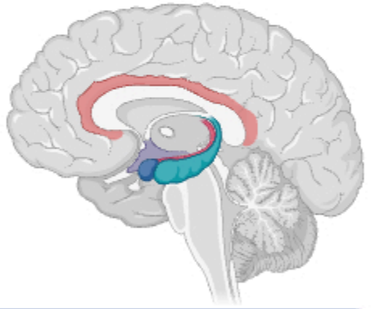

Altered brain–heart coupling in late-onset MDD

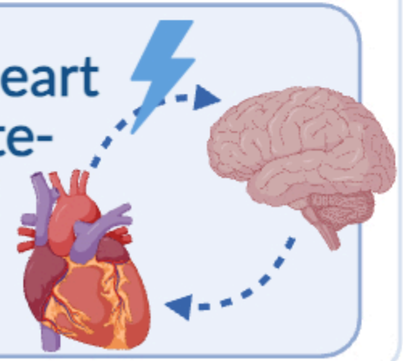

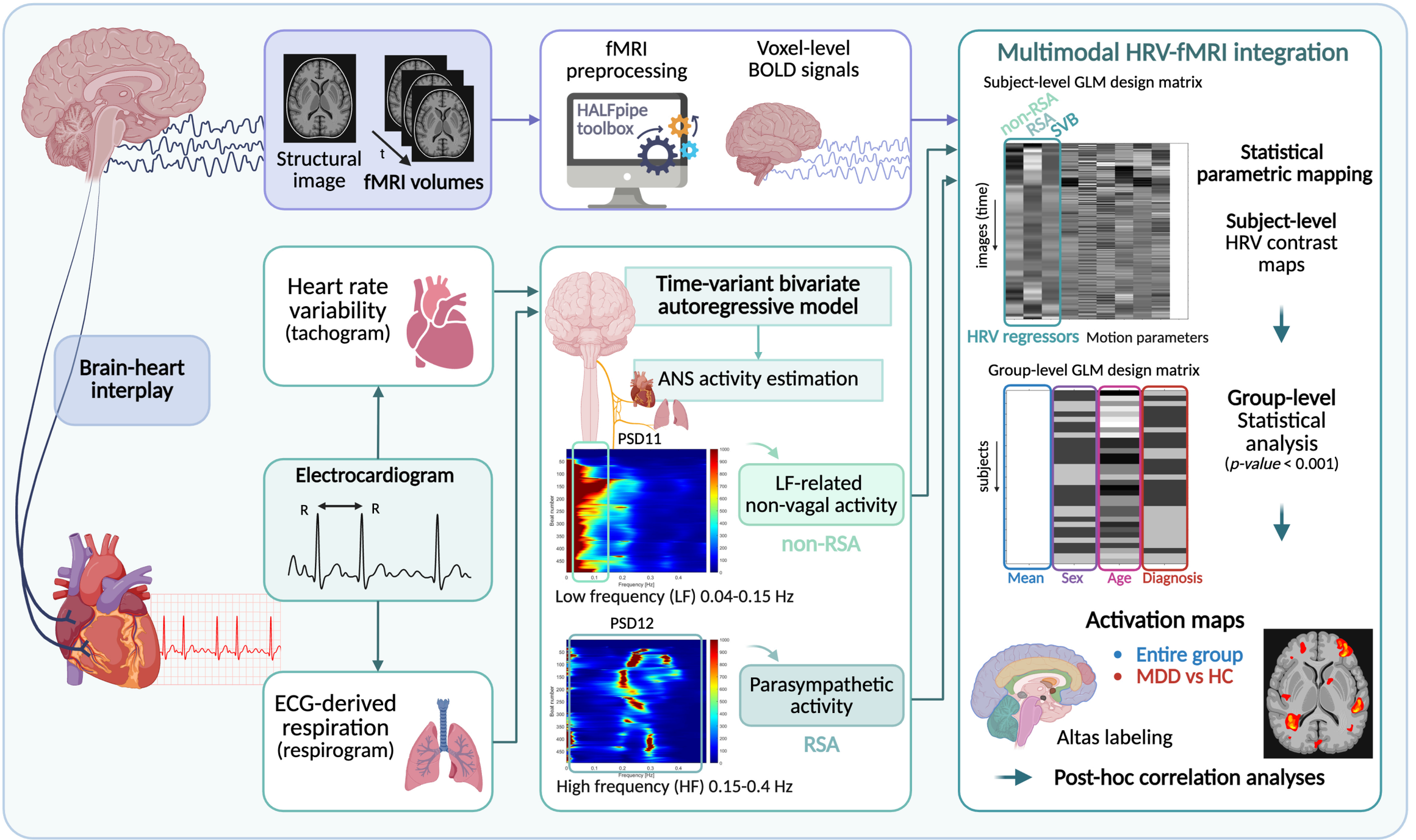
Brain-heart interplay
Structural image
t
fMRI volumes
fMRI preprocessing
HALFpipe toolbox
Voxel-level BOLD signals
Heart rate variability (tachogram)
Electrocardiogram
R
R
ECG-derived respiration (respirogram)
Time-variant bivariate autoregressive model
ANS activity estimation
PSD11
LF-related non-vagal activity
non-RSA
Low frequency (LF) 0.04-0.15 Hz
PSD12
Parasympathetic activity
RSA
High frequency (HF) 0.15-0.4 Hz
Multimodal HRV-fMRI integration
Subject-level GLM design matrix
non-RSA
RSA
SVB
images (time)
HRV regressors
Motion parameters
Statistical parametric mapping
Subject-level HRV contrast maps
Group-level GLM design matrix
subjects
Mean
Sex
Age
Diagnosis
Group-level Statistical analysis (p-value < 0.001)
Activation maps
Entire group
MDD vs HC
Altas labeling
Post-hoc correlation analyses

A Non-RSA

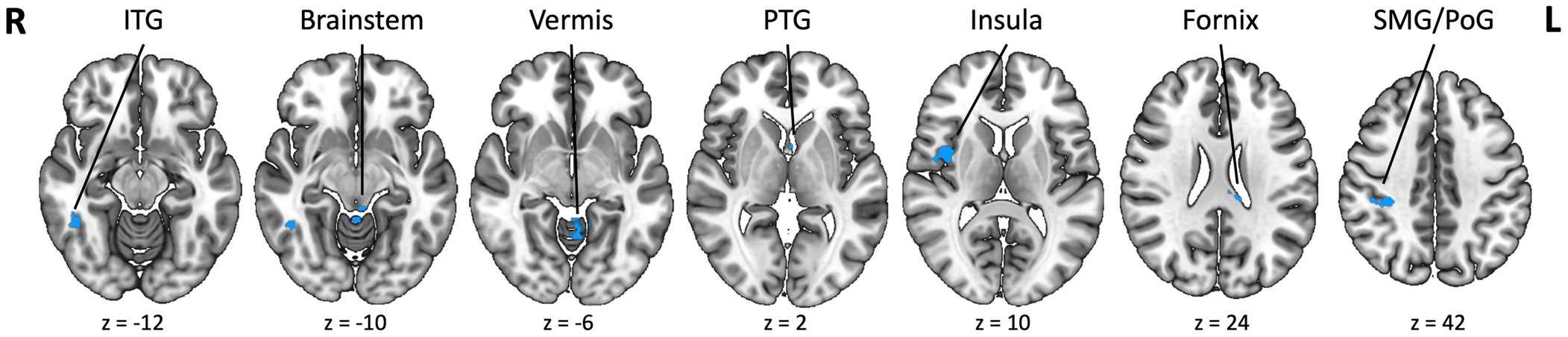

B RSA

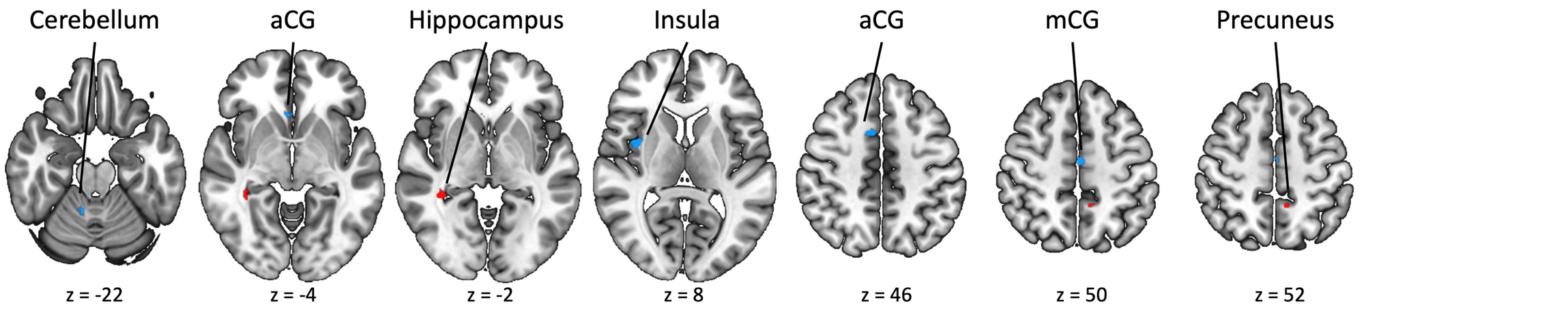

C SVB

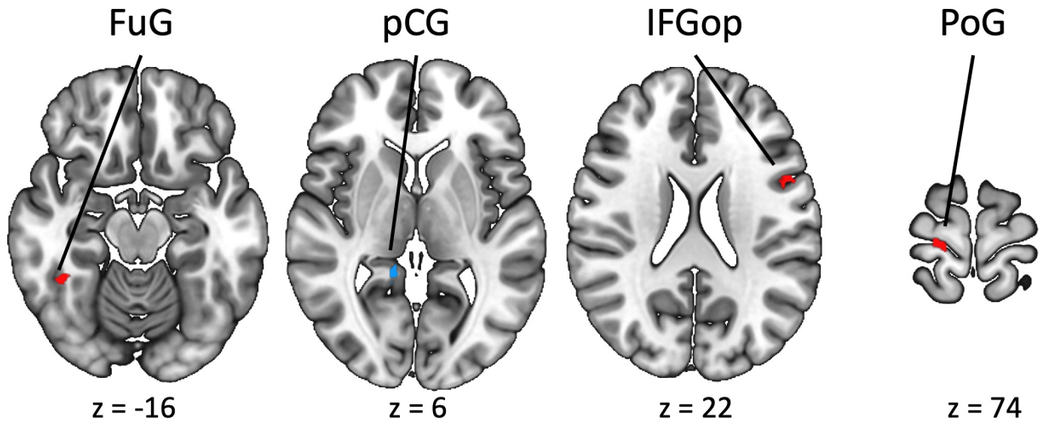

D Non-RSA vs. RSA

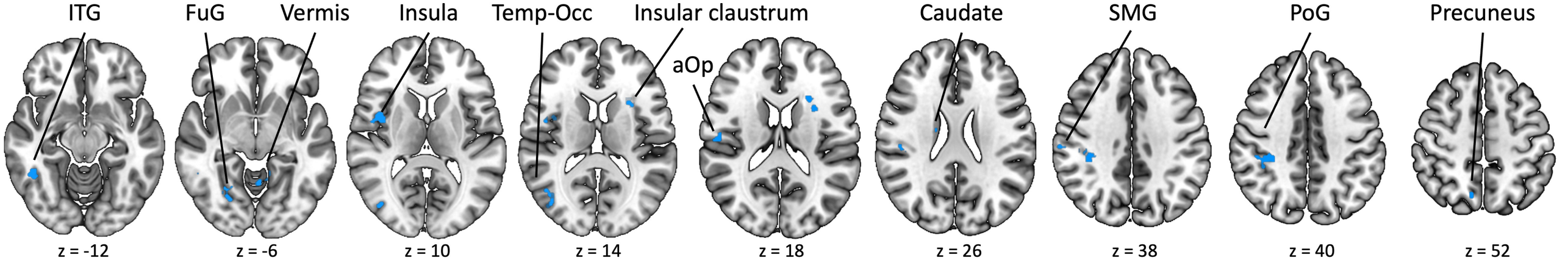

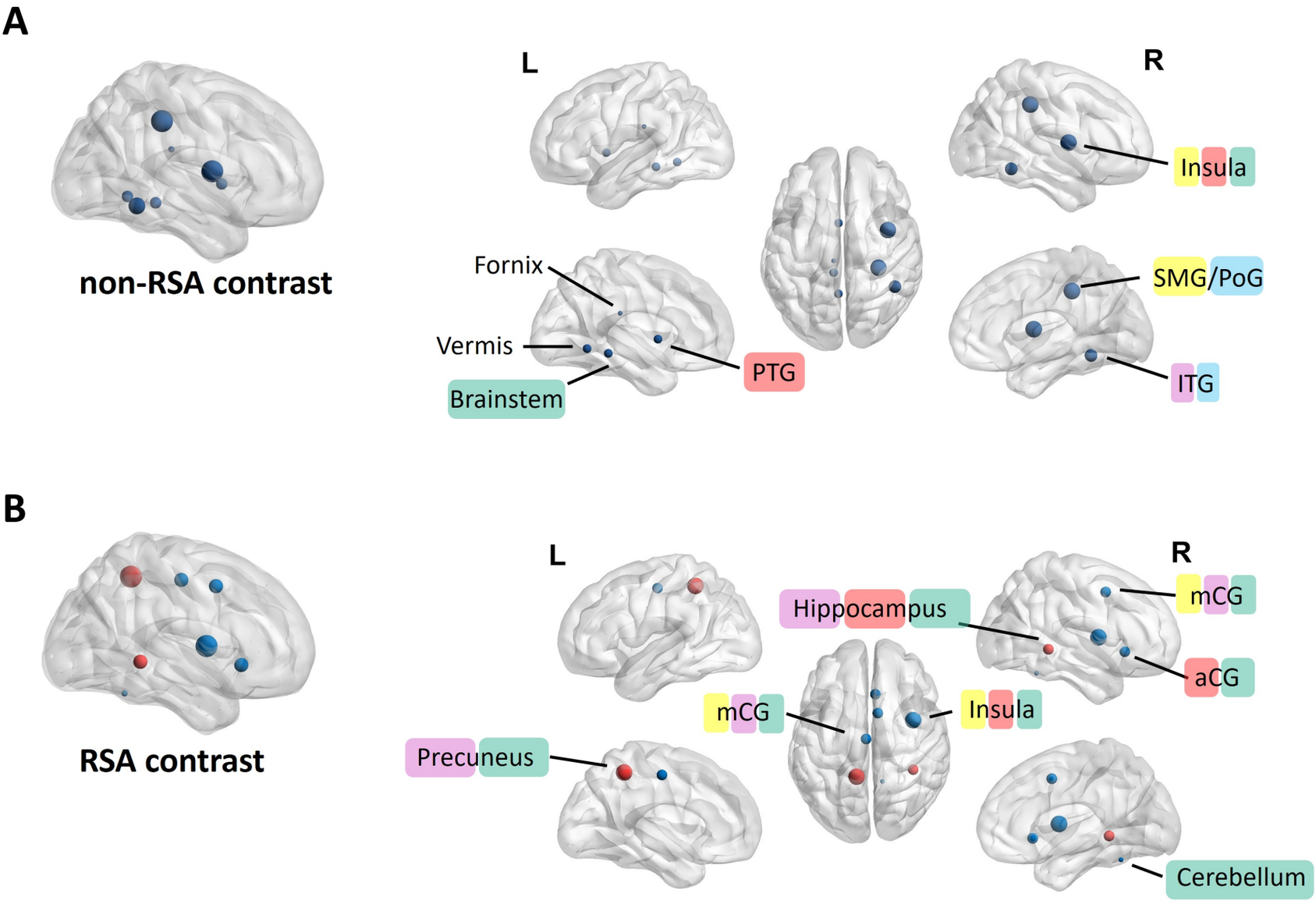
A
non-RSA contrast
L
R
Insula
Fornix
SMG/PoG
Vermis
PTG
ITG
Brainstem
B
RSA contrast
L
R
mCG
Hippocampus
aCG
mCG
Insula
Precuneus
Cerebellum
C
frontoparietal network
default mode network
ventral attention network
dorsal attention network
affective network
central autonomic network
Precuneus
mPFC
Thalamus
Insula
ACC
Hippocampus
Hypothalamus
Amygdala
Cerebellum